2017

Room-Temperature Sodium-Sulfur Batteries: A Comprehensive Review on Research Progress and Cell Chemistry

Yunxiao Wang
University of Wollongong, yunxiao@uow.edu.au

Binwei Zhang
University of Wollongong, bz370@uowmail.edu.au

Weihong Lai
University of Wollongong, wl478@uowmail.edu.au

Yanfei Xu
University of Wollongong, yx867@uowmail.edu.au

Shulei Chou
University of Wollongong, shulei@uow.edu.au

See next page for additional authors

Publication Details

Wang, Y., Zhang, B., Lai, W., Xu, Y., Chou, S., Liu, H. & Dou, S. (2017). Room-Temperature Sodium-Sulfur Batteries: A Comprehensive Review on Research Progress and Cell Chemistry. Advanced Energy Materials, 1602829-1-1602829-17.

Room-Temperature Sodium-Sulfur Batteries: A Comprehensive Review on Research Progress and Cell Chemistry

Abstract

Room temperature sodium-sulfur (RT-Na/S) batteries have recently regained a great deal of attention due to their high theoretical energy density and low cost, which make them promising candidates for application in large-scale energy storage, especially in stationary energy storage, such as with electrical grids. Research on this system is currently in its infancy, and it is encountering severe challenges in terms of low electroactivity, limited cycle life, and serious self-charging. Moreover, the reaction mechanism of S with Na ions varies with the electrolyte that is applied, and is very complicated and hard to detect due to the multi-step reactions and the formation of various polysulfides. Therefore, understanding the chemistry and optimizing the nanostructure of electrodes for RT-Na/S batteries are critical for their advancement and practical application in the future. In the present review, the electrochemical reactions between Na and S are reviewed, as well as recent progress on the crucial cathode materials. Furthermore, attention also is paid to electrolytes, separators, and cell configuration. Additionally, current challenges and future perspectives for the RT-Na/S batteries are discussed, and potential research directions toward improving RT-Na/S cells are proposed at the end.

Disciplines

Engineering | Physical Sciences and Mathematics

Publication Details

Wang, Y., Zhang, B., Lai, W., Xu, Y., Chou, S., Liu, H. & Dou, S. (2017). Room-Temperature Sodium-Sulfur Batteries: A Comprehensive Review on Research Progress and Cell Chemistry. Advanced Energy Materials, 1602829-1-1602829-17.

Authors

Yunxiao Wang, Binwei Zhang, Weihong Lai, Yanfei Xu, Shulei Chou, Hua-Kun Liu, and Shi Xue Dou

WILEY-VCH

DOI: 10.1002/ ((please add manuscript number))
Progress Reports

Room-temperature sodium-sulfur batteries: A comprehensive review on research progress and cell chemistry

Yun-Xiao Wang, Binwei Zhang, Weihong Lai, Yanfei Xu, Shu-Lei Chou,* Hua-Kun Liu, Shi-Xue Dou*

Dr. Y. X. Wang, B. W. Zhang, W. H. Lai, Y. F. Xu, Dr. S. L. Chou, Prof. H. K. Liu, Prof. S. X. Dou
Institute for Superconducting & Electronic Materials, Australian Institute of Innovative Materials, University of Wollongong, Innovation Campus, Squires Way, North Wollongong, NSW 2500, Australia

Keywords: room-temperature sodium-sulfur batteries, sulfur cathode, ether-based electrolyte, carbonate-based electrolyte, shuttle phenomenon, cell configuration

Room temperature sodium-sulfur (RT-Na/S) batteries have recently regained a great deal of attention due to their high theoretical energy density and low cost, which make them promising candidates for application in large-scale energy storage, especially in stationary energy storage, such as with electrical grids. Research on this system is currently in its infancy, and it is encountering severe challenges in terms of low electroactivity, limited cycle life, and serious self-charging. Moreover, the reaction mechanism of S with Na ions varies with the electrolyte that is applied, and is very complicated and hard to detect due to the multi-step reactions and the formation of various polysulfides. Therefore, understanding the chemistry and optimizing the nanostructure of electrodes for RT-Na/S batteries are critical for their advancement and practical application in the future. In the present review, the electrochemical reactions between Na and S are reviewed, as well as recent progress on the crucial cathode materials. Furthermore, attention also is paid to electrolytes, separators, and cell configuration. Additionally, current challenges and future perspectives for the RT-Na/S batteries are discussed, and potential research directions toward improving RT-Na/S cells are proposed at the end.

1. Introduction

Rechargeable lithium-ion batteries (LIBs) have attracted tremendous attention over the past two decades.[1-5] Given their relatively high cost, as well as their high energy and power densities, LIBs have been considered the most promising technology in small/mid-size applications such as portable devices and electric vehicles (EVs). They are not favourable power options for large-scale stationary energy storage, however, such as in electrical grids.[6-8] Various emerging energy storage systems, including lithium-air batteries,[9-16] lithium-sulfur batteries (Li/S),[11, 17-23] vanadium redox batteries,[24-31] sodium-ion batteries (SIBs),[32-40] and room-temperature sodium-sulfur (RT-Na/S) batteries,[37,41-49] are currently attracting most of the attention in the quest to power our future society.

For the aim of stationary energy storage, RT-Na/S batteries stand out due to their overwhelming advantages in terms of low cost and sufficient energy density. In contrast, Li/S batteries with high energy density and long cycle life are mainly for operation of EVs, which is considered as the most promising technologies beyond routine LIBs. Sodium, as a low-cost and abundant alternative to lithium, has driven research on Na/S technologies beyond the cell chemistry of the analogue lithium system. High-temperature sodium-sulfur batteries operated at around 300 ^{o}C with molten electrodes and a solid beta-alumina electrolyte are now commercially available. This system exhibits obvious advantages in terms of reasonable power and energy densities, temperature stability, and high efficiency with long cycle life, so that it exceeds the scale and cost requirements for grid-scale applications. [42, 50] The additional cost and high operating temperature of this technology (300-350 ^{o}C), however, directly prohibit its extensive application in EVs. [51, 52] Expensive highly alloyed steels are utilized due to the high corrosion from the liquid sodium and sulfur. Further costs are also incurred to achieve the operating temperature. In order to realize a wide range of applications, ambient temperature sodium batteries have been arousing tremendous research interest in recent years, [53] because they are much safer than commercial high-temperature Na/S and Na/$NiCl_2$ batteries, and therefore suitable for stationary grid and even transportation applications. The operation of a Na/S battery at room temperature (RT-Na/S), however, faces the critical challenge of low reversible capacity and extremely fast capacity fade during cycling. [54-58] This low capacity is likely to be due to the low electrical conductivity of S at room temperature and the formation of soluble polysulfides, which diffuse through the electrolyte to the anode and undergo redox reactions to form lower-order polysulfides at the anode surface. This shuttle phenomenon is also a common problem in Li/S batteries.[17, 59-63] Unfortunately, the shuttle effect is even exacerbated in the RT-Na/S system, resulting in low efficiency and

rapid capacity decay during cycling. All these challenges have hindered the development of reversible, sustainable, and efficient sulfur cathodes. Due to the revival of interest from 2012, research on the cell chemistry of RT-Na/S batteries is thriving. Significant progress has been achieved in terms of cycling stability, accessible capacity, Coulombic efficiency, and rate capability. Impressively, considerable efforts have been made to alleviate the shuttle effect, such as by embedding sulfur species in a functional matrix, [48, 54] separator coating/modification,[47,64-65] passivation of the anode,[56, 66] and changing the configuration of the cell. [119-129] Our overall understanding of the cell chemistry, however, is still poor, and it varies under different experimental conditions. In this review, we will present the principles and development from high-temperature to room-temperature sodium-sulfur batteries, and the technical challenges of the RT-Na/S batteries. Significant attention will be devoted to discussing our current understanding of the mechanisms operating between Na and S. As shown in **Figure 1**, we will summarize the research progress on sulfur/sodium polysulfides/sodium sulphide cathodes and sodium metal anodes. We will also focus on the selection and optimization of electrolytes, separators, and cell configurations. Overall, with the boom in research on RT-Na/S batteries, we are summarizing the vital growth in understanding of, and achievements and progress on Na/S batteries from various aspects, thereby offering a comprehensive reference for future advances in this field.

2. Principles of Sodium-sulfur batteries

2.1 Principles of high-temperature sodium-sulfur (HT-Na/S) batteries

The development of HT-Na/S batteries can be dated back to the 1960s, along with the discovery of sodium beta-alumina (β-$NaAl_{11}O_{17}$) by Kummer and his co-workers, which could serve as a high-temperature solid-state sodium ion conductor.[67] This significant discovery aroused extensive interest and led to great progress both in the field of solid state ionics and in Na/S electrochemistry.[68] Given the high conductivity of β-$NaAl_{11}O_{17}$ and the molten nature of the active electrode materials at elevated temperatures, the HT-Na/S batteries are practically operated at temperatures of 300 to 350 ^{o}C. This technology possesses obvious advantages in terms of low cost, reasonable power and energy densities, temperature stability, and high efficiency with long cycle life. Furthermore, the HT-Na/S batteries are environmentally benign, since these batteries are sealed and allow no emissions during operation. More than 99% of the overall weight of the battery materials can be recycled (the steel, copper, and aluminium). In addition to the potential hazards of sodium, [69] the safety

concerns due to the high operating temperature of this technology prohibit its further advancement and application in electrical vehicles.[51] The high operating temperature forces a fraction of the energy to be used to maintain the operating temperature, resulting in a lower overall efficiency (87 %).[52] The molten polysulfides are also proven to be corrosive to the electrode current collectors.[70] On the other hand, the solid electrolyte would gradually become fragile and eventually break during battery operation, which likely results in the risk of fire or even explosion due to the molten sodium penetration through the cell and consequent short circuits and vigorous reactions. In addition, processes for recycling the sodium and sulfur from these batteries are apparently still not developed. [71]

As shown in **Figure 2**, the HT-Na/S battery typically consists of molten Na (anode) contained within a sodium *β*-alumina tube, which acts as the solid electrolyte / separator and is surrounded by molten S (cathode). The sulfur is usually impregnated into graphite felt to give it sufficient electronic conduction to carry out the electrochemical reactions. The magnified cross-section in Figure 2 shows the transport of the Na ions through the *β*-$NaAl_{11}O_{17}$ electrolyte / separator to the S cathode during the discharge process. The Na ions then react with the S to produce various sodium polysulfide intermediates. During the subsequent charge processes, reversible reactions take place, in which the resultant sodium polysufides are reduced to S, with Na transported back into the interior of the tube. The use of light elements, Na and S, endows the Na/S system with high specific capacity and high energy density (760 Wh kg^{-1}, and not only in terms of mass, but also of volume: 2584 Wh L^{-1}). [72] For safety reasons, the commercial HT-Na/S batteries are considered to be unfavourable for transportation application in EVs, and they are exploited predominantly for stationary energy storage.[73]

The discharge process is graphically represented in **Figure 3**a. Due to its high (sodium) ionic conductivity and good insulating properties towards electrons, *β*-$NaAl_{11}O_{17}$ solid electrolyte is able to avoid self-discharge. When sodium gives off an electron, the Na^+ migrates to the sulfur container, where the electron reacts with sulfur to form sodium polysulfide (S_x^{2-}). The discharge process in the Na/S cell reactions can be described as follows:

Anode: $2Na \rightarrow 2Na^+ + 2e^-$ (1)

Cathode: $xS + 2e^- \rightarrow S_x^{2-}$ (2)

Overall reaction: $2Na + xS \rightarrow Na_2S_x$ (3)

Specifically, Okuno's group suggested that a two-phase region of sulfur and sodium polysulfide (Na_2S_5) was present at 2.075 V (**Figure 3**b), because these two liquids are

immiscible at the operating temperature. When the cell is further discharged, both S and Na_2S_5 react with Na to form a single phase region (Na_2S_4), and Na_2S_3 occurs at 1.74 V. Solid Na_2S_2 is formed at deeper discharge, which leads to increased resistance at the positive electrode and prohibits any further discharge reaction.[74] Therefore, most reports fail to achieve one-third of the theoretical gravimetric capacity of the sulfur electrode (1675 mA h g^{-1}), based on full reduction to Na_2S.[75]

High-temperature sodium–sulfur batteries have been primarily manufactured by NGK Insulators Ltd. in Japan since 2003. They are commercially available in Japan and in the United States with a discharge power capacity of ~530 MW, and are extensively applied for load leveling, peak shaving, energy arbitrage, auxiliary power, and energy storage in electrical grids.

2.2 Principles of room-temperature Na-S batteries (RT-Na/S)

Due to the great potential of the Na/S system as a high-energy power source, research on alternative ambient temperature sodium batteries is currently predominant. Typically, as shown in **Figure 4**a, RT-Na/S cells are assembled with sulfur or sulfur-containing composite applied as the cathode and paired with a sodium metal anode. A solution of organic solvents (such as ethylene carbonate / propylene carbonate: EC / PC) with sodium salts (such as $NaClO_4$) is used as the electrolyte. The assembled cells are placed in the ambient environment for electrochemical tests. During the discharge process, sodium metal is oxidized at the anode, resulting in the production of sodium ions and electrons. The sodium ions move internally to the cathode through the electrolyte, while the electrons travel to the positive electrode through the external electrical circuit, thereby generating an electrical current. Meanwhile, sulfur is reduced to produce sodium polysulfides by accepting the sodium ions and electrons at the positive electrode.

the anode and cathode reactions during charge/discharge of the RT-Na/S battery can be expressed as:

Anode: $Na \leftrightarrow Na^+ + e^-$ (4)

Cathode: $nS + 2Na^+ + 2e^- \leftrightarrow Na_2S_n$ $(4 \leq n \leq 8)$ (5)

During the discharge process, as illustrated in Figure 4b, region I represents a high-voltage plateau region at ~ 2.2 V, corresponding to a solid-liquid transition from elemental sulfur to dissolved long-chain sodium polysulfide:

$S_8 + 2Na^+ + 2e^- \rightarrow Na_2S_8$ (6)

Region II is a sloping region in the voltage range from 2.2 to 1.65 V, corresponding to a liquid-liquid reaction from the dissolved Na_2S_8 to Na_2S_4:

$Na_2S_8 + 2Na^+ + 2e^- \rightarrow 2Na_2S_4$ (7)

Region III is a low-voltage plateau region at ~1.65 V, corresponding to a liquid-solid transition from the dissolved Na_2S_4 to insoluble Na_2S_3 or Na_2S_2:

$Na_2S_4 + 2/3Na^+ + 2/3e^- \rightarrow 4/3Na_2S_3$ (8)

$Na_2S_4 + 2Na^+ + 2e^- \rightarrow 2Na_2S_2$ (9)

$Na_2S_4 + 6Na^+ + 6e^- \rightarrow 4Na_2S_2$ (10)

Region IV: A second sloping region in the range of 1.65 - 1.20 V, corresponding to a solid-solid reaction from the insoluble Na_2S_2 to Na_2S:

$Na_2S_2 + 2Na^+ + 2e^- \rightarrow 2Na_2S$ (11)

Among the four reaction regions, region II is supposed to be the most complicated one and is affected by the chemical equilibria between the various types of polysulfide species in the solution. The capacity and discharge voltage of Region III depend on the competition between Equations (8)-(10). Owing to the nonconductive nature of Na_2S_2 and Na_2S, region IV is kinetically slow and likely suffers from high polarization.[78] According to the reaction equations, the theoretical cell capacity is as high as 1672 mAh g^{-1}, offering a competitive option for low-cost, large-scale energy storage applications.

3. Technical challenges

The operation of a Na−S battery at ambient temperature, however, faces critical challenges arising from both the materials and the system.[54-58] The common theoretical and technological issues for RT-Na/S are similar to those for Li/S batteries, which mainly involve the following aspects, including (1) the low conductivity of sulfur (~10^{-30} S cm^{-1}); (2) the low reactivity between sodium and solid sulfur in liquid electrolyte; (3) the unstable electrochemical contact within the sulfur electrode, due to its structural and morphological changes related to the formation of sodium polysulfides (Na_2S_n) during charge/discharge processes; and (4) the increasing impedance resulting from the passivation of electrodes as cycling proceeds. In contrast to Li/S batteries, all these problems are intensified in RT-Na/S batteries, especially the sluggish electroactivity and rapid polysulfide migration, which make improvements on RT-Na/S batteries more difficult and challenging.

3.1 Shuttle mechanism

As we discussed above, a series of intermediate redox species would be formed during the cell operation, including high-order (Na_2S_n, $4 < n \leq 8$) and low-order (Na_2S_m, $4 < m \leq 2$) sodium polysulfides. The long-chain Na_2S_n are highly soluble in organic electrolytes with carbonate-based solvents, and they can freely migrate between cathode and anode. When the Na_2S_n migrate toward the Na anode, Na_2S_n and Na could react to produce low-order Na_2S_m polysulfides, which can form high-order Na_2S_n again during their migration back to the cathode, and so on. This process is called the shuttle phenomenon, which is also a common problem in Li/S batteries.[17, 59] Unfortunately, due to the highly reactive nature of Na, the reaction between Na and Na_2S_n species is more vigorous, and the shuttle effect is exacerbated in the RT-Na/S system, resulting in low efficiency and rapid capacity decay during cycling.

3.2 Self-discharge

Low self-discharge is an essential criterion for the practical application of various energy-storage technologies. It is a significant challenge that RT-Na/S cells feature serious self-discharge behaviour. The self-discharge occurs because the active materials gradually

dissolve. The high-order polysulfides continue to slowly dissolve in the electrolyte during the resting state and then shuttle to the sodium anode, resulting in a concentration gradient.[80]

Many strategies have been adopted in order to enhance the kinetics of the S cathode and alleviate the shuttle effect, so as to achieve high-performance RT-Na/S batteries. Most tactics focus on optimizing the S cathode by decreasing the sulfur particle size and/or confining sulfur in highly conductive matrices. Other strategies have also been explored, including constructing novel cell configurations with interlayers, assembling Na/high-ordered polysulfide cells, and utilizing efficient electrolytes. The following sections will introduce some representative examples of these approaches.

4. Cathodes

The insulating nature of cathode active materials and the polysulfide shuttle effect of RT-Na/S batteries are the major chronic problems impeding practical applications. The straightforward solution is to mix/embed/encapsulate sulfur in a suitable electrical conductor (conductive carbon/polymer). This strategy has been widely investigated, and representative research has been listed in **Table 1**, which summarizes the electrochemical performance of RT-Na/S batteries with various cathode and electrolyte compositions. So far, incorporating active materials in various carbon frameworks has provided significant enhancement of the electrochemical performance of RT-Na/S batteries.

4.1 Conventional sulfur mixture cathode

The direct solution to coping with the intrinsic low conductivity of S is to enhance the proportion of conductive additive in the cathode composition. The conductive additive, commonly consisting of carbon black, active carbon, or Super P, has the properties of high surface area and high electrical conductivity. *Via* mixing with an appropriate conductive carbon, the insulating S could be evenly distributed in the conductive framework. The sulfur utilization can thus be improved, with enhanced overall conductivity of the S cathode. The first report on the effective use of this strategy was by Park *et al.* Their cathode was composed

of 70 wt % S, 20 wt % C, and 10 wt % poly(ethylene oxide) (PEO), delivering a first discharge capacity of 489 mA h g^{-1}, but suffering from rapid capacity decay over 10 cycles. [55] Later on, this group engaged in further efforts by utilizing acetylene black as the conductive carbon with polyvinylidene fluoride (PVDF) − hexafluoropropylene gel polymer electrolyte. Similar Na-storage performance was achieved, with the first discharge capacity of 392 mA h g^{-1}, followed by higher capacity retention over 10 cycles.[57] In 2013, Wenzel *et al.* [47] increased the ratio of carbon to 40 wt %, and the cell delivered a initial discharge capacity of ~450 mA h g^{-1} with enhanced cycling stability over 40 cycles. Even though this method is straightforward and effective, it is obvious that simple physical mixing only yields disappointing accessible capacity and steep capacity decline with cycling. This is because the direct mechanical mixing only lead to poor contact between S and the conductive additives. On the other hand, a large amount of sulfur agglomerates on the carbon surface, which would block electron diffusion and transport, resulting in inferior electrochemical performance.

4.2 Sulfur-based composite cathode

4.2.1 Sulfurized polyacrylonitrile

In 2007, Wang *et al.* [54] made significant progress on RT-Na/S batteries, in which the first sulfur - conductive-polymer hybrid composite was developed. Sublimed sulfur was utilized as a dehydrogenating reagent to react with polyacrylonitrile (PAN) at 300 ^{o}C. During the thermal treatment, an S-PAN compound, composed of π-conjugated ring structures covalently bonded to S species, is formed via the cyclization of the –CN groups in PAN polymer. Extra S is believed to be uniformly dispersed and stabilized in the composite. The resultant cell delivered a high capacity of 500 mA h g^{-1} with stable cycling over 18 cycles. Later on, a higher heating temperature of 450 ^{o}C was applied to an S-PAN nanofiber (NF) mixture,[58] which was fabricated via the electrospinning method (**Figure 5**a). Significant enhancement was achieved; as displayed in Figure 5b, the S could react with the PAN-derived carbon matrix (c-PAN) and form covalent bonds with the C atoms, forming the final c-PAN sulfur (c-

PANS) composite. The atomic arrangements of S in the C matrix were proven to be responsible for the stable cycling of the obtained c-PANS composite, which exhibited high initial charge/discharge capacities of 250 and 364 mA h g^{-1} (Figure 5c). Significantly, the structure of the c-PANS composite was robust, leading to prolonged cycling stability over 500 cycles and high rate performance (Figure 5d). In addition, this material can be utilized to construct a flexible Na/S battery. Kim *et al.* [81] prepared S-PAN webs via the same method, which was directly utilized as cathode without the addition of conductive carbon and binder. The S-PAN/Na cell delivered a high first charge capacity of 1473 mA h g^{-1}, and a capacity of 266 mA h g^{-1} was retained over 200 cycles. The enhancement was mainly ascribed to the chemical binding between S and the C framework, which could effectively suppress polysulfide dissolution and realize high electrochemical activity between S and Na.

4.2.2 Sulfur - carbonaceous composite cathode

More efforts have been devoted to engineering various composite configurations via incorporating a high ratio of S into carbonaceous matrices. The frequently used carbon materials include microporous carbon (pore size < 2 nm), mesoporous carbon (2 nm < pore size < 50 nm), hollow carbon spheres, macroporous carbon (pore size > 50 nm), graphene, and carbon nanotubes (CNTs). Each type of carbonaceous matrix possesses unique morphological advantages. The micropores are favourable for accommodating and immobilizing the active materials. The mesoporous carbon with larger pore size could realize high sulfur loading and improve sodium ion and electrolyte transport. The macropores usually can ensure excellent electrolyte immersion. In addition, CNT networks with various micro/meso/macropores can be fabricated, which are expected to show improved cycling performance.

For the fabrication of sulfur-carbonaceous composite, the melt-diffusion method is extensively utilized to load various amount of S into the carbonaceous matrices. The obtained

composites can confine the S in the matrixes and guarantee intimate contact between them, thereby immobilizing the active material and enhancing the sulfur utilization. The free space and pores in the carbon matrices also can trap the dissolved polysulfides, blocking the serious shuttle effect. Furthermore, these nanostructures are believed to absorb/channel the liquid electrolyte.

4.2.2.1 S-carbon nanotube (CNT) composite

The CNTs function as an extensively interwoven conductive network in the S cathode in lithium-sulfur batteries. Xin *et al.* [82] optimized this S-based composite via coating a microporous carbon (~ 0.5 nm) layer on the CNTs (S/CNT@MPC), and the small sulfur allotropes S_{2-4} were successfully confined in the microporous carbon. Owing to the high electroactivity of S_{2-4} and the confinement by the microporous carbon, the S/CNT@MPC cathode showed superior electrochemical performance in a Li-S battery. Later on, the same group applied this S/CNT@MPC cathode in RT-Na/S batteries.[48] As illustrated in **Figure 6**a, the small sulfur molecules (S_{2-4}) can be well confined in the carbon micropores (0.5 nm). Meanwhile, the supposed products, Na_2S_2 and Na_2S molecules, possess denser and more flattened structures, which can be accommodated by the carbon micropores with similar diameters. Due to the complete reaction with Na to Na_2S, a high specific capacity of 1610 mA h g^{-1} was delivered, which is very close to the theoretical capacity (1675 mA h g^{-1}) of Na/S batteries. Without the formation of high-order sodium polysulfides, the cell no longer suffers from the destructive effects of the shuttle phenomenon, thus realizing stable cycling capability and maintaining high capacity. The composite in Figure 6b showed a reversible capacity of ~ 500 mA h g^{-1} over 200 cycles and high-rate capability of ~ 815 mA h g^{-1} at 2 C (1 C = 1670 mA h g^{-1}).

4.2.2.2 S-hollow carbon sphere composite

In order to address the challenges of serious polysulfide solubility and slow kinetics, Lee *et al.*[83] explored hollow carbon spheres as an effective S host. The hollow carbon spheres are synthesized by the hydrothermal method, and they possess a large diameter of ~1000 nm. As suggested by the researchers, the interior void space of the hollow carbon can accommodate a large amount of active elemental sulfur, guaranteeing a high sulfur loading rate in the composite. On the other hand, the carbon shell is capable of confining the starting active sulfur and polysulfides in its interior space, thereby inhibiting the occurrence of the shuttle effect. Furthermore, the carbon shell ensures high lithium ion and electron transport. The composite showed a discharge plateau around 1.3 V and delivered a reversible capacity of ~ 600 mA h g^{-1} over 20 cycles. It should be pointed out that the size of the hollow carbon spheres is expected to be reduced to the nanoscale in the future, which is likely to suppress the formation of inactive sulfur cores when sulfur fills the hollow spaces, enhancing electron transport and thereby achieving higher accessible capacity and sustainable cycling.

More recently, Wang *et al.* [80] explored interconnected mesoporous carbon hollow nanospheres (*i*MCHS) as a highly effective host, in which the size of the carbon nanospheres was ~100 nm, with enormous mesopores in the carbon shell (~ 10 nm). The obtained composite of S with interconnected mesoporous carbon hollow nanospheres delivered high capacity retention of ~ 88.8% over 200 cycles and superior rate capability. Significantly, the mesoporous carbon shells can work as open active diffusion channels for ions, electrons, and electrolyte, and efficiently block the polysulfide shuttle. Moreover, apart from encapsulation in the hollow spaces, a certain amount of sulfur can be embedded in the carbon mesopores, which can localize the polysulfides. In addition, based on *in situ* synchrotron X-ray diffraction, the mechanism of the room temperature Na/S battery is proposed to be reversible reactions between S_8 and Na_2S_4, corresponding to a theoretical capacity of 418 mAh g^{-1}.

4.2.2.3 S-(Cu-decorated) mesoporous carbon composite

With the assistance of Cu nanoparticles, Zheng *et al.* [84] confirmed the feasibility of high-surface-area mesoporous carbon (HSMC) as an excellent S host. The synergistic effects of nano-Cu decoration and the mesoporous C host were responsible for the exceptional performance of the HSMC-Cu-S. The nano-Cu inclusions are believed to play a key role in the significant enhancement of electrochemical properties. The Cu nanoparticles are able to immobilize S through the strong interaction between Cu and S. Meanwhile, the addition of Cu could enhance the overall electronic conductivity of the cathode. More importantly, the mesopores are supposed to provide free space for the volume changes of S during charge/discharge processes. The HSMC-Cu-S cathode exhibited a reversible capacity of ~ 610 mA h g^{-1} up to 110 cycles with a Coulombic efficiency of 100 %.

4.2.2.4 S-carbonized metal-organic framework composite

A significant achievement was reported by Archer's group.[85] A metal-organic framework (MOF)-derived microporous carbon polyhedral host (cMOF) was fabricated using a zeolite-type MOF (zeolitic imidazolate framework: ZIF-8) carbonized in flowing N_2 gas, which possesses small micropores, high surface area, and good affinity of carbon for S. As shown in **Figure 7**a, the S was successfully infused into cMOF via heating the S and cMOF mixture at 155 ^oC for 2 h and then further heating at 300 ^oC for 6 h. It was demonstrated that the cMOF could provide strong physical confinement and immobilization for both S and the resultant polysulfides. The cell was proven to undergo solid-state electrochemical reactions with the S confined in the micropores, leading to a high reversible capacity of 600 mA h g^{-1} and nearly 100% Coulombic efficiency (Figure 7b). Meanwhile, in Chen *et al.*'s work,[86] a S-cZIF composite was synthesized via heating the mixture at 155 ^oC for 12 h. With a similar S loading ratio of ~ 50 wt % but different electrolyte (1 M of $NaClO_4$ in tetraethylene glycol dimethyl ether: TEGDME), the cell manifested higher capacity and longer cycling life than those for Archer's group, delivering a reversible specific capacity of ~ 1000 mA h g^{-1} at 0.1 C and maintaining 500 mA h g^{-1} at 0.2 C after 250 cycles. This was because of the synergistic

effects between the C matrix and the high N-doping (~ 18 at %). This work also confirmed the confinement and immobilization of S molecules inside the carbon matrix.

4.3 Sodium polysulfide/sulfide cathodes

4.3.1 Na_2S_6-MWCNT composites

As shown in **Figure 8**a, Yu *et al.* [76] synthesized long-chain sodium polysulfide (Na_2S_6) as a cathode for RT-Na/S batteries. Using liquid-phase Na_2S_6 instead of S as the cathode ensures a homogeneous distribution in the conductive matrix and high electrochemical activity. On the other hand, this work is a unique approach to understanding the Na-storage mechanism of the ambient-temperature Na-S battery system. The self-weaving multiwall carbon nanotubes (MWCNT) act as a high-surface-area current collector to construct the binder-free electrode. The Na_2S_6/MWCNT cathode retained a capacity of ~ 400 mA h g^{-1} over 30 cycles. Besides acting as the carbon matrix and current collector, the MWCNT fabric electrode also works as a trapping interlayer (Figure 8b and c). Later on, as shown in Figure 8c and d, Yu *et al*. further developed this Na_2S_6 polysulfide catholyte cathode with a composite matrix of activated carbon (AC) dispersed into the interwoven carbon nanofiber fabric (CNF/AC) with a sodiated Nafion® membrane as the ion-selective separator.[87] Significantly, the non-porous sodiated Nafion membrane offers both sufficient Na ion conductivity and decreased sodium polysulfide permeation, exhibiting remarkably high capacity of ~ 600 mA h g^{-1} with excellent cycling stability over 200 cycles.

4.3.2 Na_2S-C composites

Similarly, Yu *et al.* also carried out a series of studies on the Na_2S cathode, which allows the utilization of sodium-free anodes for room-temperature sodium-sulfur batteries, with the possibilities including hard carbon, metal oxides, Sn, and Si. In 2015, they were the first to report the electrochemical performance of a Na_2S cathode. The Na_2S slurry was made from Na_2S powder, short MWCNTs, and tetraethylene glycol dimethyl ether (TEGDME) solvent. After magnetic stirring, the Na_2S-MWCNT cathode could be obtained by injecting the Na_2S

slurry into the self-weaving, binder-free MWCNT fabric. The Na/S batteries with the Na_2S/MWCNT cathode exhibited remarkable capacity of 650 mAh g^{-1} after 50 cycles at the current density of 167 mA g^{-1}.[88] Furthermore, Yu *et al.* optimized Na ‖ Na-Nafion/AC−CNF coating ‖ Na_2S/AC−CNF cells in a coin-cell configuration (CR2032).[89] For the Na_2S cathode, the activated carbon nanofiber (AC-CNF) was utilized to form a self-weaving and free-standing paper matrix. Novel modified Nafion membranes were utilized as the separator. This separator was enhanced by sodiation and coated by the AC-CNF material, which was effective for suppressing the polysulfide shuttle effect and for both the electrochemical utilization of the sulfur cathode and the preconditioning of the cell, thereby delivering reversible capacity of ~ 600 mA h g^{-1} with enhanced cyclability of the cell (100 cycles).

5. Anodes

Almost all the research has exploited sodium metal as anode, which possesses an extremely high theoretical capacity (1166 mAh g^{-1}) and low redox potential. It is well known that Na metal anode in liquid electrolytes poses safety concerns. Non-uniform nucleation of Na at the anode leads to the formation of Na dendrites during cycling, which might pierce the separator to internally short-circuit the cell. On the other hand, on exposure to the liquid electrolyte, the fresh sodium metal might react with the solvent, leading to low Coulombic efficiency, non-uniform ionic flux, and large Na dendrites. Lee *et al.* [83] reported the utilization of a Na-Sn-C alloy anode, which could improve the cycling stability, but sacrificed the overall output voltage of the RT-Na/S batteries. Cui's group[90] reported a simple liquid electrolyte to achieve highly reversible and non-dendritic plating-stripping of Na anode at room temperature. The electrolyte was $NaPF_6$ in glymes (mono-, di-, and tetraglyme), in which uniform protective solid electrolyte interphase (SEI) films consisting of inorganic Na_2O and NaF could be generated on the surface of the Na metal. Surprisingly, the SEI films are impermeable to the electrolyte and conducive to non-dendritic Na growth. Most recently, ionic liquid 1-methyl-3-propylimidazolium-chlorate tethered to SiO_2 nanoparticles (SiO_2-IL-ClO_4 particles)

as an additive in liquid carbonate electrolytes has been proven to play a specific role in Na anode protection. The additives serve as an agent to stabilize electrodeposition, and further investigations are expected to fully explain the protective mechanism of SiO_2-IL-ClO_4.[85] High safety and high energy-density RT-Na/S batteries are expected to be achieved with the significant development of the Na metal anode.

6. Advances in the electrolyte, separator, and cell configuration

Electrolytes offer ion transport pathways between the anode and the cathode. The selection of the electrolyte directly determines the RT-Na/S battery performance. Typically, a solid-state electrolyte is favorable to alleviate the dissolution of polysulfides and the shuttle phenomenon. The utilization of solid electrolyte, however, is challenging due to the low ionic conductivity and interfacial instability. For liquid electrolyte, more attention needs to be paid to the severe solubility of intermediate polysulfides. The investigation of various electrolytes is imperative to determine the optimal electrolyte composition for enhanced electrochemical performance of RT-Na/S batteries.

Separators can physically block electrical contact between the anode and cathode, while maintaining the ion diffusion in the electrolyte. In addition, it is essential for separators to possess high mechanical strength and flexibility in case they are pierced, leading to battery failure. For RT-Na/S batteries, ion selective separators have become more promising due to their action towards reducing the polysulfide shuttle.

According to the experience on Li-S batteries, the cell configuration of RT-Na/S cells was modified by introducing a bifunctional interlayer between the separator and the cathode, which can work well to prevent internal short circuits, while permitting sodium ion diffusion. More importantly, the interlayer can effectively localize the migration of polysulfides within the cathode region of the cell and protect the sodium metal anode, leading to long-term cycling stability with high sulfur utilization.

6.1 Electrolytes

6.1.1 Polymer/solid-state electrolyte

During the initial stages of research, non-aqueous polymer-based gels were used in RT-Na/S batteries, including $NaCF_3SO_3$-polyvinylidene fluoride (PVDF)-tetraglyme,[91] $NaCF_3SO_3$-poly(ethylene oxide) (PEO),[55] $NaCF_3SO_3$-PVDF-hexafluoropropylene (HFP)-tetraglyme,[92] and $NaCF_3SO_3/SiO_2$ − ethylene carbonate (EC) − propylene carbonate (PC)-(PVDF-HFP).[93] This type of electrolyte could effectively avoid the potential fire hazard, although the cells tended to deliver low capacity and rapid cycling decay , which were due to the poor dimensional stability, low ionic conductivity, and poor interfacial stability of the polymer-based gels. Beta-alumina, as a solid-state electrolyte, is commercially available and possesses a high ionic conductivity of ~ 2 mS cm^{-1}. As illustrated in **Figure 9**a and b, beta-alumina was placed between the two half cells and applied as a separator by Wenzel *et al.* [47] The electrolyte consisted of 1 M $NaCF_3SO_3$ in a mixture of 1,3-dioxolane (DOL) /dimethoxyethane (DME). Glass fiber was utilized for the separator. This strategy was verified to prevent the diffusion of polysulfides towards the sodium electrode. More recent progress was made by Kim *et al.* on a high S ratio cathode (~ 60 %), and they further studied a hybrid electrolyte made by combining beta-alumina and a liquid electrolyte consisting of 1 M $NaCF_3SO_3$ in TEGDME. [94] As shown in Figure 9c, what they found was that the high-order sodium polysulfides (Na_2S_n, $4 \leq n \leq 8$) could be confined in the sulfur cathode area by using the hybrid electrolyte. They also believe that the high voltage region, corresponding to the formation of the high-order sodium polysulfides, is associated with the cycling stability, while the low voltage region, associated with the formation of solid-state Na_2S_m ($1 \leq m \leq 3$), is responsible for the capacity fade. This RT-Na/S battery showed a high first discharge capacity (855 mA h g^{-1}), good cycling performance (100 cycles), and high Coulombic efficiency (close to 100%).

6.1.2 Ether-based electrolyte

Various ether solvents have been investigated as one of the most promising candidate types for Li/S batteries.[95-98] Compared with small-molecule ethers, the long-chain analogs show favorable electrochemical performance, due to their high boiling/flash points, non-flammability, and stability at high potentials. Among them, TEGDME showed the best electrochemical properties in Li/S batteries, with beneficial effects due to the greater solvation of oxygen atoms in the glyme structure, thereby solubilizing and dissociating the Li salts and polysulfide compounds.[98]

The investigation of liquid electrolyte solvents for RT-Na/S started with ethers, including DOL/DME, TEGDME, and tetraglyme. Studies suggested that the ether-based electrolytes are likely to contribute to low capacity.[41, 55, 65] Although the theoretical end product Na_2S could be detected, the capacity was only about 350-550 mA h g^{-1}, indicating that the sodiation reaction is incomplete, with the production of an overall composition of Na_2S_x ($3 \leq x \leq 5$). The charge/discharge plateaus occur at ~1.85 V, which is close to the overall expected cell potential. The low achieved capacity is due to the high solubility of high-order polysulfides in the ether-based electrolyte. As discharge proceeds, more and more dissolved polysulfides shuttle to the anode side, leading to less formation of low-order polysulfides. The cells with ether-based electrolyte, therefore, undergo a severe shuttle effect and strong self-discharge, leading to low capacity and fast capacity decay.

6.1.3 Carbonate-based electrolyte

Carbonate solvents commonly possess high ionic conductivity and wide electrochemical stability, while offering favorable anode passivation. According to the results in Li/S batteries, however, carbonates can react with reduced-solubility polysulfides through a possible nucleophilic attack on the carbonate molecules during the initial discharge process, resulting in degradation of the electrolyte, loss of active sulfur, and sudden capacity failure. [99,100] On the other hand, carbonate-based electrolytes have been used successfully in Li/S batteries

when the S is completely encapsulated or covalently immobilized in the host materials / polymeric composites. [82, 101-105]

Carbon-based electrolytes, such as $NaClO_4$ in EC/dimethyl carbonate (DMC) and $NaClO_4$ in EC/PC, are commonly investigated in RT-Na/S batteries.[48,54,58,76,82] It is interesting that the voltage profiles of these cells with the carbonate-based electrolyte are very different from those with ether-based electrolytes.[41] The cells usually display continuously decreasing profiles during subsequent cycling, and much of the capacity is obtained below 1.5 V, which indicates a different reaction mechanism to that in the ether-based electrolyte. High-order polysulfides are formed and irreversibly react with the carbonate electrolyte in RT-Na/S batteries as well.[106, 107] Similarly, considerable work has been focused on embedding the S in a C host, and in this case, the cathode coupled with carbonate electrolyte undergoes a solid-state reaction without the formation of soluble intermediate polysulfides in Na-S batteries. Wang *et al.* and Hwang *et al.* demonstrated that sulfur confined in PAN-based materials can work well with EC/DMC electrolyte.[54, 58] Xin *et al.* [49] showed that EC/PC electrolyte can be used in cells with short-chain sulfur molecules of S_{2-4} embedded in a narrow microporous carbon matrix. Recently, Wei *et al.* [85] significantly optimized the compatibility of S cathode with carbonate electrolyte via immobilization of the S in a microporous C matrix and utilization of ionic liquid combined with the liquid carbonate electrolyte.

6.1.4 Ionic-liquid-based electrolyte

Room-temperature ionic liquids (ILs) are composed entirely of ions, which favorably possess negligible volatility, low flammability, high thermal stability, acceptable conductivity, and a wide electrochemical potential window. These advantages have promoted the study of ILs as electrolytes in Li/S batteries.[108-112] Until now, research on ILs in RT-Na/S has been very rare. Very recently, Wei *et al.* [85] utilized 1-methyl-3-propylimidazolium-chlorate ionic-liquid-tethered silica nanoparticle (SiO_2–IL–ClO_4) additive as an agent in a carbonate-based electrolyte (1 M $NaClO_4$ in EC/PC). The electrochemical performance suggested that the ILs

are capable of stabilizing the cell. The tethered ILs are favorable for forming a robust and stable solid electrolyte interphase (SEI) film on the sodium anode surface, which prevents the occurrence of side reactions with the electrolyte.[113] Meanwhile, the SiO_2 particles can anchor ClO_4^- anions, which serve as supporting electrolyte, thus reducing the electric field through the tethered anion effect.[114, 115]

6.2 Separator

Polypropylene and glass fiber separators are commonly used in RT-Na/S batteries. The high-order polysulfide intermediates in Na/S batteries are likely to diffuse into the separators during charge/discharge processes, and then preferentially precipitate as inactive S-related species on the surface of the S cathode. [116] The micron-scale pores of the polypropylene separators and of glass fiber separators are definitely not able to prevent the permeation of the sodium polysulfides. Through surface modification, the functionalized membranes lead to enhanced specific capacity and cycling stability. Based on the effective tactic of constructing permselective separators for Li/S batteries,[117-120] research efforts on RT-Na/S batteries are shifting to ionic separators as well. Obvious shuttle suppression was achieved by Bauer *et al.*,[65] who presented for the first time a polysulfide inhibiting separator that was made by coating a thin layer of Nafion on a conventional polypropylene separator. This cation selective separator prohibits the diffusion of polysulfide anions through the separator, thereby demonstrating alleviation of the polysulfide shuttle, efficient operation, and good cycling stability. Furthermore, Yu *et al.* exploited non-porous sodiated Nafion membrane as a Na-ion exchange separator,[87, 89] which demonstrated high ionic conductivity of 2.7×10^{-5} S cm^{-1} at room temperature. Thus, the Na-Nafion separator provided favorable Na^+-ion conductivity. As illustrated in **Figure 10**a, the Nafion membrane consists of a hydrophobic region and a hydrophilic ion-cluster region (~ 4-5 nm). These hydrophilic clusters are connected to each other through hydrophilic channels (~ 1-2 nm). Significantly, with its $–SO^{3-}$ groups at the hydrophilic “pore” surface, the Nafion membrane offers a negatively charged environment,

so that it works as an excellent cation-exchange membrane (Figure 10b). Therefore, this membrane can suppress the sodium polysulfide migration through the "structure effect" and the "electronic effect" at the fine hydrophilic nanopores (< 5 nm).[89] These cells with Nafion membranes exhibited remarkably high energy density and cycling stability.

6.3 Cell configuration

As mentioned above, the RT-Na/S batteries suffer from an accelerated shuttle effect, so the traditional cell configuration might be unsuitable and incompatible with this system. Based on the research achievements in Li/S batteries, cell configuration modification has been regarded as an effective strategy to optimize cell performance through improvements in terms of the S loading and active material utilization ratio. In particular, the use of an interlayer could perfectly solve the problem of polysulfide migration, and such interlayers have been extensively applied in the Li/S cell configuration.[120-122]

This concept has been imported into the RT-Na/S technologies. Manthiram's group developed the interlayer strategy for the S cathode. Similarly, the interlayer could confine the dissolved sodium polysulfide on the cathode side and enhance the electroactivity of the cathode. This interlayer, therefore, leads to less shuttle effect and better capacity retention. In contrast to the traditional RT-Na/S cells (**Figure 11**a)**,** the interlayer in Figure 11b is typically placed between the cathode and separator as a polysulfide-diffusion inhibitor. It has been confirmed that the interlayer can effectively capture/localize the migrating polysulfides within the cathode region of the cell, leading to high S utilization and prolonged cycling stability. On the other hand, the interlayers should be highly conductive, which can enhance the conductivity of pure sulfur cathodes and promote the re-utilization of the trapped active materials. Various carbonaceous materials, therefore, have been employed as interlayers, including micro/mesoporous carbon,[120, 123, 124] interwoven CNFs/CNTs, [121, 125, 126] porous metal foam, [127] carbon paper, [128] and porous biomaterials. [129, 130]

As shown in Figure 11c, a carbon nano-foam interlayer consisting of carbon nanofibers was placed between the separator and the sulfur cathode. The conductive interlayer can localize the soluble polysulfide species and prevent their migration to the anode. On the other hand, it also acts as a secondary current collector to capture the polysulfide species by electrochemical deposition during charge/discharge processes. It is obvious that the capacity with the functional interlayer is much higher than that without the interlayer over 20 cycles (Figure 11d).[77] Moreover, they investigated the impact of three interlayers, including a CNF thin film and a CNT thin film, as well as commercially available carbon foams (CCFs).[78] The nanostructures of these interlayers could come into direct contact with the S cathode, which reduces the electrical resistance and facilitates electrolyte penetration during charge/discharge processes. The cell with the CNT interlayer showed low initial discharge capacity due to the poor wettability of the CNTs by the electrolyte. Over 20 cycles, all the cells with various interlayers showed similar cycling performance, with remarkable capacity of 400 mAh g^{-1} and energy density of 720 W h kg^{-1} based on sulfur mass, which is a significant enhancement compared to the conventional cell configurations.[54-56, 91-93] Nevertheless, it should be pointed out that the high capacity retention of the RT-Na/S with this configuration is realized at the expense of energy density, being the same problem as is encountered in using additional separators. Further work on elaborately regulating the weight and thickness of the interlayer should be deployed to balance the energy density and cycling stability.

7. Conclusions and Perspectives

In this review of research progress, we have considered the development from high-temperature to room-temperature Na/S batteries, emphasizing a comprehensive understanding of RT-Na/S batteries, including the essential principles, associated technical challenges, and significant progress to date. We have mainly focused on the latest advances in cathode materials, which are the most essential and critical factor for a leap in performance of RT-Na/S batteries.

By developing functional nanocomposites, utilizing efficient electrolytes, and constructing novel cell configurations, research on the RT-Na/S system is booming, and significant breakthroughs have been achieved in recent years. Nanostructured composites, such as S-microporous carbon, Na_2S_8-CNT, and Na_2S-CNT nanocomposites, have been intensively pursued over recent years. The introduction of a C matrix can directly enhance the overall conductivity of the cathode. The nanoscale composites are able to facilitate rapid ion/electron transport. More importantly, the porous C matrix is capable of trapping the polysulfide intermediates. This type of cathode has achieved superior performance in terms of high capacity, good rate capability, and prolonged cycling stability. Furthermore, the selection of the electrolyte plays an important role in coping with the polysulfide migration in RT-Na/S batteries. For example, the high-order polysulfide species are highly soluble in TEGDME-based electrolyte but insoluble in EC/PC-based electrolyte. Some subtle factors, including the solubility of polysulfides in the electrolyte and the competition between the affinity of S towards the C matrix and towards the electrolyte, determine whether and what intermediate species are present. In ether-based electrolytes, the charge/discharge curves show similarity to those in Li/S cells; but the cells only deliver low capacities and rapid cycling decay. A different mechanism is deduced when carbonate-based electrolyte is used. The voltage profiles are much less defined, and the carbonates might react with polysulfides, as in the case of Li/S batteries. Much higher capacity and long cycle life can be achieved. The electrochemistry of RT-Na/S, therefore, is very complicated, and advanced characterization techniques are required to provide a better understanding of the Na-storage mechanisms. Moreover, cell configuration modification plays a critical role in improving the performance of RT-Na/S batteries. Currently, it only involves the utilization of an interlayer. A favorable impact has been achieved *via* the confinement effect of the interlayer, which could localize the polysulfides and prevent the occurrence of the shuttle phenomenon, effectively addressing the challenges of low active material utilization and high self-charging.

In comparison to Li/S batteries, the study on RT-Na/S batteries has not been fully deployed and literally involves the above-mentioned fundamental research. Much effort should be made to catch up with the pace of Li/S batteries in the near future. The low sulfur elelctroactivity and accelerated shuttle phenomenon are the critical issues to tackle in RT-Na/S batteries. Currently, nanostructured metal oxides and sulfides have been confirmed as favourable S host in Li/S batteries, which have showed superior ability to optimize S cathode with high sulfur utilization and prolonged cycling life. The effects of metal oxides and sulfides have been speculated by experimental results and theoretical calculation, which are closely related to their conductivity, adsorption ability to polysulfides, elecatalytic capability, and affinity to polysulfides.[131] Regarding S cathode in RT-Na/S batteries, great attention should be paid to these two types of matrices, which includes to explore suitable host materials and investigate the corresponding conversion mechanism of soluble polysulfides and insoluble (di)sulfides. Meanwhile, it is profound to compare and understand the different Na-storage mechanisms when various host materials and electrolytes are applied. In the future, more research efforts are expected towards the design of unique sandwich-structured electrodes and the use of porous current collectors. Separator modification, e.g., Na-Nafion® coatings on Celgard®, could significantly suppress the polysulfide shuttle, thereby improving the capacity and cyclability of the RT-Na/S cells. In addition, efforts towards developing safe anode materials are imperative as well, which involve exploring alternative protected sodium metal anodes, Na/M (M = metal) alloys, and favorable electrolytes as a feasible approach to build safer RT-Na/S batteries.

Even with these intensified efforts and even though the RT-Na/S batteries have made great progress since 2012, the research on RT-Na/S batteries is still in its infancy, and it will be a long process to realize their practical applications. Future efforts should be guided by the rich experience on Li/S batteries and towards basic scientific research and approaches.

Acknowledgements

This research was financially funded by the Australian Research Council (ARC) (DE170100928, LP120200432, DP140104062, and DP160102627), the Commonwealth of Australia through the Automotive Australia 2020 Cooperative Research Centre (Auto CRC), and the Baosteel-Australia Joint Research and Development Center (Baosteel Grant no. BA14006). We acknowledge the use of the facilities at the UOW Electron Microscopy Centre funded by ARC grants (LE0882813 and LE0237478). We also thank Dr. Tania Silver for critical reading of the manuscript.

Received: ((will be filled in by the editorial staff))
Revised: ((will be filled in by the editorial staff))
Published online: ((will be filled in by the editorial staff))

[1] B. Dunn, H. Kamath, J.-M. Tarascon, *Science* **2011**, *334*, 928.

[2] M. Armand, J. M. Tarascon, *Nature* **2008**, *451*, 652.

[3] J.-M. Tarascon, M. Armand, *Nature* **2001**, *414*, 359.

[4] A. Manthiram, *J. Phys. Chem. Lett.* **2011**, *2*, 176.

[5] J. B. Goodenough, Acc. Chem. Res. **2013**, *46*, 1053.

[6] V. Etacheri, R. Marom, R. Elazari, G. Salitra, D. Aurbach, *Energy Environ. Sci.* **2011**, 4, 3243.

[7] J. B. Goodenough, K. S. Park, *J. Am. Chem. Soc.* **2013**, *135*, 1167.

[8] B. Scrosati, J. Garche, *J. Power Sources* **2010**, *195*, 2419.

[9] T. Ogasawara, A. Débart, M. Holzapfel, P. Novák, P. G. Bruce, J *J. Am. Chem. Soc.* **2006**, *128*, 1390.

[10] G. Girishkumar, B. McCloskey, A. Luntz, S. Swanson, W. Wilcke, *J. Phys. Chem. Lett.* **2010**, *1*, 2193.

[11] P. G. Bruce, S. A. Freunberger, L. J. Hardwick, J. M. Tarascon, *Nat. Mater.* **2012**, *11*, 19.

[12] F. Y. Cheng, J. Chen, Chem. *Soc. Rev.* **2012**, *41*, 2172.

[13] S. A. Freunberger, Y. H. Chen, N. E. Drewett, L. J. Hardwick, F. Barde, P. G. Bruce, *Angew. Chem.-Int. Edit.* **2011**, *50*, 8609.

[14] J. S. Lee, S. T. Kim, R. Cao, N. S. Choi, M. Liu, K. T. Lee, J. Cho, *Adv. Energy Mater.* **2011**, *1*, 34.

[15] Y. C. Lu, Z. C. Xu, H. A. Gasteiger, S. Chen, K. Hamad-Schifferli, Y. Shao-Horn, *J. Am. Chem. Soc.* **2010**, *132*, 12170.

[16] Z. Q. Peng, S. A. Freunberger, Y. H. Chen, P. G. Bruce, *Science* **2012**, 337, 563.

[17] X. Ji, K. T. Lee, L. F. Nazar, *Nat. Mater.* **2009**, *8*, 500.

[18] J. C. Guo, Y. H. Xu, C. S. Wang, *Nano Lett.* **2011**, *11*, 4288.

[19] N. Jayaprakash, J. Shen, S. S. Moganty, A. Corona, L. A. Archer, *Angew. Chem.-Int. Edit.* **2011**, *50*, 5904.

[20] C. D. Liang, N. J. Dudney, J. Y. Howe, *Chem. Mater.* **2009**, *21*, 4724.

[21] B. Zhang, X. Qin, G. R. Li, X. P. Gao, *Energy Environ. Sci.* **2010**, *3*, 1531.

[22] G. Y. Zheng, Y. Yang, J. J. Cha, S. S. Hong, Y. Cui, *Nano Lett.* **2011**, *11*, 4462.

[23] Y.-X. Wang, L. Huang, L.-C. Sun, S.-Y. Xie, G.-L. Xu, S.-R. Chen, Y.-F. Xu, J.-T. Li, S.-L. Chou, S.-X. Dou, *J. Mater. Chem.* **2012**, *22*, 4744.

[24] L. Y. Li, S. Kim, W. Wang, M. Vijayakumar, Z. M. Nie, B. W. Chen, J. L. Zhang, G. G. Xia, J. Z. Hu, G. Graff, J. Liu, Z. G. Yang, *Adv. Energy Mater.* **2011**, *1*, 394.

[25] Y. Y. Shao, X. Q. Wang, M. Engelhard, C. M. Wang, S. Dai, J. Liu, Z. G. Yang, Y. H. Lin, *J. Power Sources* **2010**, *195*, 4375.

[26] J. Y. Xi, Z. H. Wu, X. P. Qiu, L. Q. Chen, *J. Power Sources* **2007**, *166*, 531.

[27] A. Z. Weber, M. M. Mench, J. P. Meyers, P. N. Ross, J. T. Gostick, Q. Liu, *J. Appl. Electrochem.* **2011**, *41*, 1137.

[28] M. Ulaganathan, V. Aravindan, Q. Yan, S. Madhavi, M. Skyllas‐Kazacos, T. M. Lim, *Adv. Mater. Interfaces* **2016**, *3*, 1500309.

[29] X. F. Li, H. M. Zhang, Z. S. Mai, H. Z. Zhang, I. Vankelecom, *Energy Environ. Sci.* **2011**, *4*, 1147.

[30] M. Skyllas-Kazacos, M. H. Chakrabarti, S. A. Hajimolana, F. S. Mjalli, M. Saleem, *J. Electrochem. Soc.* **2011**, *158*, R55.

[31] A. Z. Weber, M. M. Mench, J. P. Meyers, P. N. Ross, J. T. Gostick, Q. H. Liu, *J. Appl. Electrochem.* **2011**, *41*, 1137.

[32] Y.-X. Wang, S.-L. Chou, H.-K. Liu, S.-X. Dou, Carbon 2013, 57, 202.

[33] Y.-X. Wang, Y.-G. Lim, M.-S. Park, S.-L. Chou, J. H. Kim, H.-K. Liu, S.-X. Dou, Y.-J. Kim, *J. Mater. Chem. A* **2014**, *2*, 529.

[34] Y.-X. Wang, K. H. Seng, S.-L. Chou, J.-Z. Wang, Z. Guo, D. Wexler, H.-K. Liu, S.-X. Dou, *Chem. Comm.* **2014**, *50*, 10730.

[35] B. L. Ellis, W. R. M. Makahnouk, Y. Makimura, K. Toghill, L. F. Nazar, Nat. Mater. 2007, 6, 749.

[36] S. W. Kim, D. H. Seo, X. H. Ma, G. Ceder, K. Kang, *Adv. Energy Mater.* **2012**, *2*, 710.

[37] S. Komaba, W. Murata, T. Ishikawa, N. Yabuuchi, T. Ozeki, T. Nakayama, A. Ogata, K. Gotoh, K. Fujiwara, *Adv. Funct. Mater.* **2011**, *21*, 3859.

[38] V. Palomares, P. Serras, I. Villaluenga, K. B. Hueso, J. Carretero-Gonzalez, T. Rojo, *Energy Environ. Sci.* **2012**, *5*, 5884.

[39] H. L. Pan, Y. S. Hu, L. Q. Chen, *Energy Environ. Sci.* **2013**, *6*, 2338.

[40] M. D. Slater, D. Kim, E. Lee, C. S. Johnson, *Adv. Funct. Mater.* **2013**, *23*, 947.

[41] P. Adelhelm, P. Hartmann, C. L. Bender, M. Busche, C. Eufinger, J. Janek, *Beilstein J. Nanotech.* **2015**, *6*, 1016.

[42] K. B. Hueso, M. Armand, T. Rojo, *Energy Environ. Sci.* **2013**, *6*, 734.

[43] C. W. Park, J. H. Ahn, H. S. Ryu, K. W. Kim, H. J. Ahn, *Electrochem. Solid State Lett.* **2006**, *9*, A123.

[44] C. W. Park, H. S. Ryu, K. W. Kim, J. H. Ahn, J. Y. Lee, H. J. Ahn, *J. Power Sources* **2007**, *165*, 450.

[45] H. Ryu, T. Kim, K. Kim, J. H. Ahn, T. Nam, G. Wang, H. J. Ahn, *J. Power Sources* **2011**, *196*, 5186.

[46] J. S. Kim, H. J. Ahn, I. P. Kim, K. W. Kim, J. H. Ahn, C. W. Park, H. S. Ryu, *J. Solid State Electrochem.* **2008**, *12*, 861.

[47] S. Wenzel, H. Metelmann, C. Raiss, A. K. Durr, J. Janek, P. Adelhelm, *J. Power Sources* **2013**, *243*, 758.

[48] S. Xin, Y. X. Yin, Y. G. Guo, L. J. Wan, *Adv. Mater.* **2014**, *26*, 1261**.**

[49] N. Yabuuchi, K. Kubota, M. Dahbi, S. Komaba, *Chem. Rev.* **2014**, *114*, 11636.

[50] J. Sudworth, A. Tiley, Sodium Sulphur Battery, *Springer Science & Business Media*, **1985**.

[51] A. Bito, Overview of the sodium-sulfur battery for the IEEE Stationary Battery Committee, *Power Engineering Society General Meeting*, **2005**.

[52] S. S. Berbano, I. Seo, C. M. Bischoff, K. E. Schuller, S. W. Martin, *J. Non-Cryst. Solids* **2012**, *358*, 93.

[53] M. D. Slater, D. Kim, E. Lee, C. S. Johnson, *Adv. Funct. Mater.* **2013**, *23*, 947.

[54] J. Wang, J. Yang, Y. Nuli, R. Holze, *Electrochem. Comm.* **2007**, *9*, 31.

[55] C.-W. Park, H.-S. Ryu, K.-W. Kim, J.-H. Ahn, J.-Y. Lee, H.-J. Ahn, *J. Power Sources* **2007**, *165*, 450.

[56] H. Ryu, T. Kim, K. Kim, J.-H. Ahn, T. Nam, G. Wang, H.-J. Ahn, *J. Power Sources* **2011**, *196*, 5186.

[57] J.-S. Kim, H.-J. Ahn, I.-P. Kim, K.-W. Kim, J.-H. Ahn, C.-W. Park, H.-S. Ryu, *J. Solid State Electrochem.* **2008**, *12*, 861.

[58] T. H. Hwang, D. S. Jung, J.-S. Kim, B. G. Kim, J. W. Choi, *Nano Lett.* **2013**, *13*, 4532.

[59] G. He, X. Ji, L. Nazar, *Energy Environ. Sci.* **2011**, *4*, 2878.

[60] M. R. Busche, P. Adelhelm, H. Sommer, H. Schneider, K. Leitner, J. Janek, *J. Power Sources* **2014**, *259*, 289.

[61] X. Yang, L. Zhang, F. Zhang, Y. Huang, Y. S. Chen, *Acs Nano* **2014**, *8*, 5208.

[62] Y. Yang, G. Y. Zheng, Y. Cui, *Energy Envir. Sci.* **2013**, *6*, 1552.

[63] Y. V. Mikhaylik, J. R. Akridge, *J. Electrochem. Soc.* **2004,** *151*, A1969.

[64] I. Bauer, S. Thieme, J. Brückner, H. Althues, S. Kaskel, *J. Power Sources* **2014**, *251*, 417.

[65] I. Bauer, M. Kohl, H. Althues, S. Kaskel, *Chem. Comm.* **2014**, *50*, 3208.

[66] M. Kohl, F. Borrmann, H. Althues, S. Kaskel, *Adv. Energy Mater.* **2016**, *6*, 1502185.

[67] Y.-F. Y. Yao and J. Kummer, J. *Inorg. Nucl. Chem*. **1967**, *29*, 2453IN12467.

[68] Z. Yang, J. Zhang, M. C. Kintner-Meyer, X. Lu, D. Choi, J. P. Lemmon, J. Liu, *Chem. Rev.* **2011**, *111*, 3577.

[69] Z. Wen, Y. Hu, X. Wu, J. Han, Z. Gu, *Adv. Funct. Mater.* **2013**, *23*, 1005.

[70] X. Lu, B. W. Kirby, W. Xu, G. Li, J. Y. Kim, J. P. Lemmon, V. L. Sprenkle, Z. Yang, *Energy Environ. Sci.* **2013**, *6*, 299.

[71] J. Sullivan, L. Gaines, *Energy Convers. Manage.* **2012**, *58*, 134.

[72] F. Cheng, J. Liang, Z. Tao, J. Chen, *Adv. Mater.* **2011**, *23*, 1695.

[73] M. M. Thackeray, C. Wolverton, E. D. Isaacs, *Energy Environ. Sci.* **2012**, *5*, 7854.

[74] T. Oshima, M. Kajita, A. Okuno, *Int. J Appl. Ceram. Tec.* **2004**, *1*, 269.

[75] B. L. Ellis, L. F. Nazar, *Curr. Opin. Solid State Mater. Sci.* **2012**, *16*, 168.

[76] X. Yu, A. Manthiram, *J. Phys. Chem. C* **2014**, *118*, 22952.

[77] X. Yu, A. Manthiram, *J. Phys. Chem. Lett.* **2014**, *5*, 1943.

[78] X. Yu, A. Manthiram, *Chem. Electro. Chem.* **2014**, *1*, 1275.

[79] A. Manthiram and X. Yu, *Small*, **2015**, 11, 2108.

[80] Y.-X. Wang, J. Yang, W. Lai, S.-L. Chou, Q. Gu, H. K. Liu, D. Zhao, S. X. Dou, *J. Am. Chem. Soc.* **2016**, 138,16576.

[81] I. Kim, C. H. Kim, S. hwa Choi, J.-P. Ahn, J.-H. Ahn, K.-W. Kim, E. J. Cairns, H.-J. Ahn, *J. Power Sources* **2016**, *307*, 31.

[82] S. Xin, L. Gu, N.-H. Zhao, Y.-X. Yin, L.-J. Zhou, Y.-G. Guo, L.-J. Wan, *J. Am. Chem. Soc*. **2012**, *134*, 18510.

[83] D.-J. Lee, J.-W. Park, I. Hasa, Y.-K. Sun, B. Scrosati, J. Hassoun, *J. Mater. Chem. A* **2013**, *1*, 5256.

[84] S. Zheng, P. Han, Z. Han, P. Li, H. Zhang, J. Yang, *Adv. Energy Mater.* **2014**, *4*, 1400482.

[85] S. Wei, S. Xu, A. Agrawral, S. Choudhury, Y. Lu, Z. Tu, L. Ma, L. A. Archer, *Nat. Comm.* **2016**, *7*, 11722.

[86] Y.-M. Chen, W. Liang, S. Li, F. Zou, S. M. Bhaway, Z. Qiang, M. Gao, B. D. Vogt, Y. Zhu, *J. Mater. Chem. A* **2016**, *4*, 12471.

[87] X. Yu, A. Manthiram, *Adv. Energy Mater.* **2015**, *5*, 1500350.

[88] X. Yu, A. Manthiram, *Chem. Eur. J.* **2015**, *21*, 4233.

[89] X. Yu, A. Manthiram, *Chem. Mater.* **2016**, *28*, 896.

[90] Z. W. Seh, J. Sun, Y. Sun and Y. Cui, *ACS Central Sci.* **2015**, 1, 449.

[91] C.-W. Park, J.-H. Ahn, H.-S. Ryu, K.-W. Kim, H.-J. Ahn, *Electrochem. Solid State Lett.* **2006**, *9*, A123.

[92] J.-S. Kim, H.-J. Ahn, I.-P. Kim, K.-W. Kim, J.-H. Ahn, C.-W. Park, H.-S. Ryu, *J. Solid State Electrochem.* **2008**, *12*, 861.

[93] D. Kumar, M. Suleman, S. Hashmi, *Solid State Ionics* **2011**, *202*, 45.

[94] I. Kim, J.-Y. Park, C. H. Kim, J.-W. Park, J.-P. Ahn, J.-H. Ahn, K.-W. Kim, H.-J. Ahn, *J. Power Sources* **2016**, *301*, 332.

[95] H.-S. Ryu, H.-J. Ahn, K.-W. Kim, J.-H. Ahn, K.-K. Cho, T.-H. Nam, J.-U. Kim, G.-B. Cho, *J. Power Sources* **2006**, *163*, 201.

[96] Y.-X. Wang, S.-L. Chou, H.-K. Liu, S.-X. Dou, *J. Power Sources* **2013**, *244*, 240.

[97] S.-E. Cheon, K.-S. Ko, J.-H. Cho, S.-W. Kim, E.-Y. Chin, H.-T. Kim, *J. Electrochem. Soc.* **2003**, *150*, A796.

[98] C. Barchasz, J.-C. Leprêtre, S. Patoux, F. Alloin, *Electrochim. Acta* **2013**, *89*, 737.

[99] J. Gao, M. A. Lowe, Y. Kiya, H. c. D. Abruña, *J. Phys. Chem. C* **2011**, *115*, 25132.

[100] T. Yim, M.-S. Park, J.-S. Yu, K. J. Kim, K. Y. Im, J.-H. Kim, G. Jeong, Y. N. Jo, S.-G. Woo, K. S. Kang, *Electrochim. Acta* **2013**, *107*, 454.

[101] Z. Zhang, Z. Li, F. Hao, X. Wang, Q. Li, Y. Qi, R. Fan, L. Yin, *Adv. Funct. Mater.* **2014**, *24*, 2500.

[102] H. B. Wu, S. Wei, L. Zhang, R. Xu, H. H. Hng, X. W. D. Lou, *Chem. Eur. J.* **2013**, *19*, 10804.

[103] S. Zheng, Y. Chen, Y. Xu, F. Yi, Y. Zhu, Y. Liu, J. Yang, C. Wang, *ACS Nano* **2013**, *7*, 10995.

[104] L. Yin, J. Wang, F. Lin, J. Yang, Y. Nuli, *Energy Environ. Sci.* **2012**, *5*, 6966.

[105] A. Konarov, D. Gosselink, T. N. L. Doan, Y. Zhang, Y. Zhao, P. Chen, J. *Power Sources* **2014**, *259*, 183.

[106] T. Yim, M.-S. Park, J.-S. Yu, K. J. Kim, K. Y. Im, J.-H. Kim, G. Jeong, Y. N. Jo, S.-G. Woo, K. S. Kang, I. Lee, Y.-J. Kim, *Electrochim. Acta* **2013**, *107*, 454.

[107] S. Wei, L. Ma, K. E. Hendrickson, Z. Tu, L. A. Archer, *J. Am. Chem. Soc.* **2015**, 137, 12143.

[108] J.-W. Park, K. Ueno, N. Tachikawa, K. Dokko, M. Watanabe, *J. Phys. Chem. C* **2013**, *117*, 20531.

[109] B. Guo, T. Ben, Z. Bi, G. M. Veith, X.-G. Sun, S. Qiu, S. Dai, *Chem. Comm.* **2013**, *49*, 4905.

[110] È. Boros, M. J. Earle, M. A. Gîlea, A. Metlen, A.-V. Mudring, F. Rieger, A. J. Robertson, K. R. Seddon, A. A. Tomaszowska, L. Trusov, *Chem. Comm.* **2010**, *46*, 716.

[111] K. Ueno, J.-W. Park, A. Yamazaki, T. Mandai, N. Tachikawa, K. Dokko, M. Watanabe, *J. Phys. Chem. C* **2013**, *117*, 20509.

[112] C. Zhang, A. Yamazaki, J. Murai, J.-W. Park, T. Mandai, K. Ueno, K. Dokko, M. Watanabe, *J. Phys. Chem. C* **2014**, *118*, 17362.

[113] Y. Lu, K. Korf, Y. Kambe, Z. Tu, L. A. Archer, *Angew. Chem. Int. Ed.* 2014, 53, 488.

[114] M. D. Tikekar, L. A. Archer, D. L. Koch, *J. Electrochem. Soc.* **2014**, 161, A847.

[115] Z. Tu, P. Nath, Y. Lu, M. D. Tikekar, L. A. Archer, *Acc. Chem. Res.* **2015**, 48, 2947.

[116] H. Yao, K. Yan, W. Li, G. Zheng, D. Kong, Z. W. Seh, V. K. Narasimhan, Z. Liang, Y. Cui, *Energy Environ. Sci.* **2014**, *7*, 3381.

[117] J.-Q. Huang, Q. Zhang, H.-J. Peng, X.-Y. Liu, W.-Z. Qian and F. Wei, *Energy Environ. Sci.* **2014,** 7, 347.

[118] J.-Q. Huang, T.-Z. Zhuang, Q. Zhang, H.-J. Peng, C.-M. Chen and F. Wei, *ACS Nano*, **2015**, 9, 3002.

[119] Y. Pan, Y. Zhou, Q. Zhao, Y. Dou, S. Chou, F. Cheng, J. Chen, H. K. Liu, L. Jiang and S. X. Dou, *Nano Energy*, **2017**, 33, 205.

[120] Y.-S. Su, A. Manthiram, *Nat. Comm.* **2012**, *3*, 1166.

[121] C. Zu, Y.-S. Su, Y. Fu, A. Manthiram, *Phys. Chem. Chem. Phys.* **2013**, *15*, 2291.

[122] Y.-S. Su, A. Manthiram, *Chem. Comm.* **2012**, *48*, 8817.

[123] Y. S. Su, Y. Fu, B. Guo, S. Dai, A. Manthiram, *Chem. Eur. J.* **2013**, 19, 8621.

[124] Y.-S. Su, Y. Fu, T. Cochell, A. Manthiram, *Nat. Comm.* **2013**, 4, 2985.

[125] S.-H. Chung, A. Manthiram, *Chem. Comm.* **2014**, 50, 4184;

[126] C. Zu, A. Manthiram, *Adv. Energy Mater.* **2014**, 4, 1400897.

[127] K. Zhang, F. R. Qin, J. Fang, Q. Li, M. Jia, Y. Q. Lai, Z. A. Zhang, J. Li, *J. Solid State Electrochem.* **2014**, 18, 1025.

[128] K. Zhang, Q. Li, L. Y. Zhang, J. Fang, J. Li, F. R. Qin, Z. A. Zhang, Y. Q. Lai, *Mater. Lett.* **2014**, 121, 198.

[129] S. H. Chung, A. Manthiram, *Adv. Mater.* **2014**, 26, 1360;

[130] S.-H. Chung, A. Manthiram, *ACS Sustainable Chem. Eng.* **2014**, 2, 2248.

[131] X. Liu, J.-Q Huang, Q. Zhang, L. Mai, *Adv. Mater.* **2017**, 1601759.

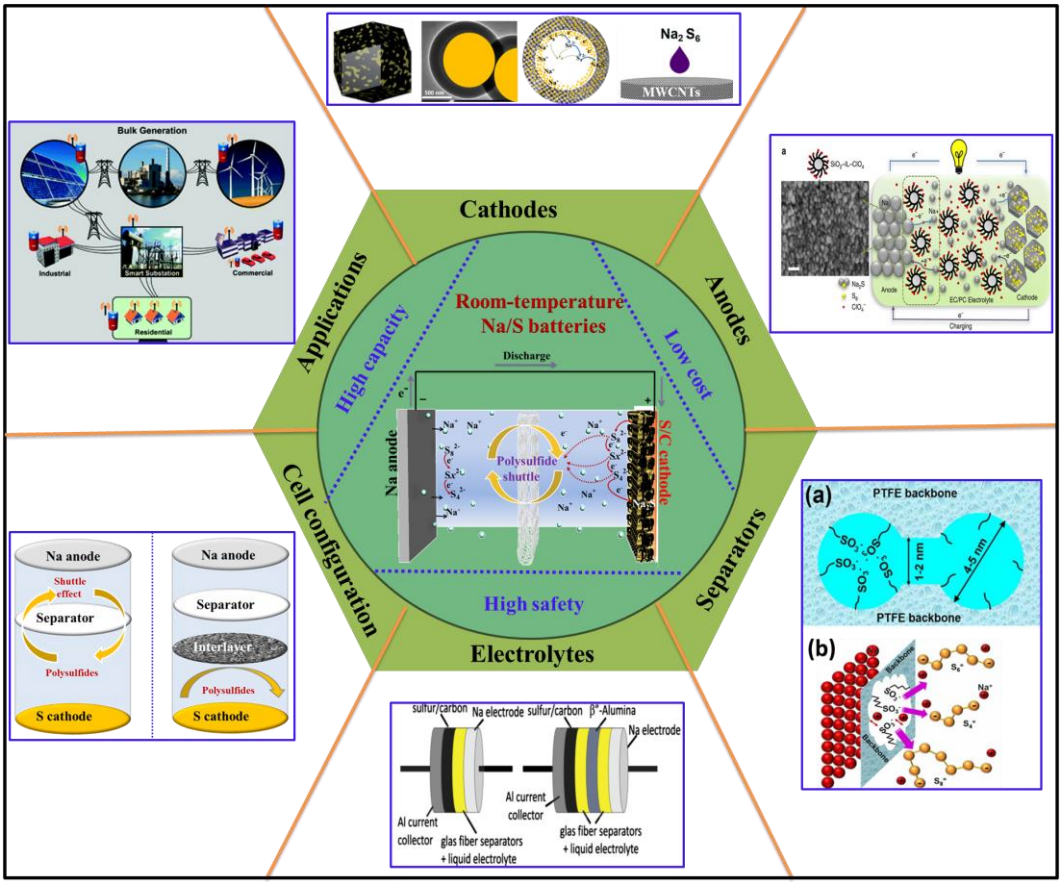

Figure 1. An overview diagram showing the advantages and applications for, and extensive research interest on cathodes, anodes, separators, electrolytes, and cell configurations. Advantages include the natural abundance and environmental benignity of S and Na. Potential applications are focused on stationary energy storage: Reproduced with permission.[68] Copyright 2011, American Chemical Society. Cathode images: Reproduced with permission.[85] Copyright 2014, Royal Society of Chemistry. Reproduced with permission.[83]Copyright 2013, Royal Society of Chemistry. Reproduced with permission.[80] Copyright 2016, American Chemical Society. Reproduced with permission.[76] Copyright 2014, American Chemical Society. Anode images: Reproduced with permission.[85] Copyright 2016, Nature Publishing Group. Separator images: Reproduced with permission.[89] Copyright 2016, American Chemical Society. Electrolyte images: Reproduced with permission.[47] Copyright 2013, Elsevier.

Table 1. Cathode composition, electrolyte composition, and electrochemical performance of RT-Na/S batteries with various cathodes that are reported in the literature.

Cathode [a]	Electrolyte [b]	Current density	1st cycle capacity (mA h/g)	Capacity (mA h/g) after (n) cycles	References
70 wt. % S 20 wt. % C 10 wt. % PEO	$NaCF_3SO_3$ in PVDF-TEGDME	No data	489	105 (10)	[91]
50 wt. % S 40 wt. % C 10 wt. % PVDF	1 M $NaCF_3SO_3$ in DOL/DME	0.148 mA cm^{-2}	450	75 (40)	[47]
70 wt. % S-PAN 20 wt. % C 10 wt. % PTFE	1 M $NaClO_4$ in EC/DMC	0.1 mA cm^{-2}	654.8	500 (18)	[54]
70 wt. % c-PANS 15 wt. % Super P 15wt. % PVDF	0.8 M $NaClO_4$ in EC/EMC	220 mA g^{-1}	364	150 (500)	[58]
0 wt. % S/CNT@MPC 10 wt. % CB 10 wt. % PVDF	1 M $NaClO_4$ in PC/EC	3340 mA g^{-1}	1610	500(200)	[82]
60 wt. % S-hollow carbon 20 wt. % C 20 wt. % PEO	$NaCF_3SO_3$ in TEGDME	167 mA g^{-1}	1000	600 (20)	[83]
70 wt. % S@*i*MCHS 10 wt. % CB 20 wt. % CMC	1 M $NaClO_4$ in EC/ PC+FEC	100 mA g^{-1}	328.4	292 (200)	[80]
80 wt. % S/Cu-decorated mesoporous C 10 wt. % C 10 wt. % CMC	1.0 M $NaClO_4$ in EC/ DMC	50 mA g^{-1}	718	641 (110)	[84]
80 wt.% MCPS 10 wt. % CB 10 wt. % PVDF	1 M $NaClO_4$ In EC/PC	84 mA g^{-1}	689	354 (100)	[85]
Na_2S_6-MWCNTs fabric cathode	1.5 M $NaClO_4$ + 0.3 M $NaNO_3$ in TEGDME	No Data	~935	400(30)	[76]
Na_2S-C nanotube Fabric cathode	1.5 M $NaClO_4$ + 0.3 M $NaNO_3$ in TEGDME	167	~850	560(50)	[88]

[a] PEO: polyethylene oxide, PVDF: polyvinylidene fluoride, PTFE: polytetrafluoroethylene, PAN: polyacrylonitrile, CNT@MPC: carbon nanotube core@microporous carbon shell, iMCHS: interconnected mesoporous carbon hollow nanospheres, CMC: carboxymethyl cellulose, MCPS: S/microporous carbon polyhedron composite, MWCNTs: multiwall carbon nanotubes. [b] $NaCF_3SO_3$: sodium triflate, $NaClO_4$: sodium perchlorate, $NaNO_3$: sodium nitrate, TEGDME: tetraethylene glycol dimethyl ether, DOL: 1,3-dioxolane, DME: dimethoxyethane, EC: ethylene carbonate, DMC: dimethyl carbonate, PC: propylene carbonate, FEC: fluoroethylene carbonate.

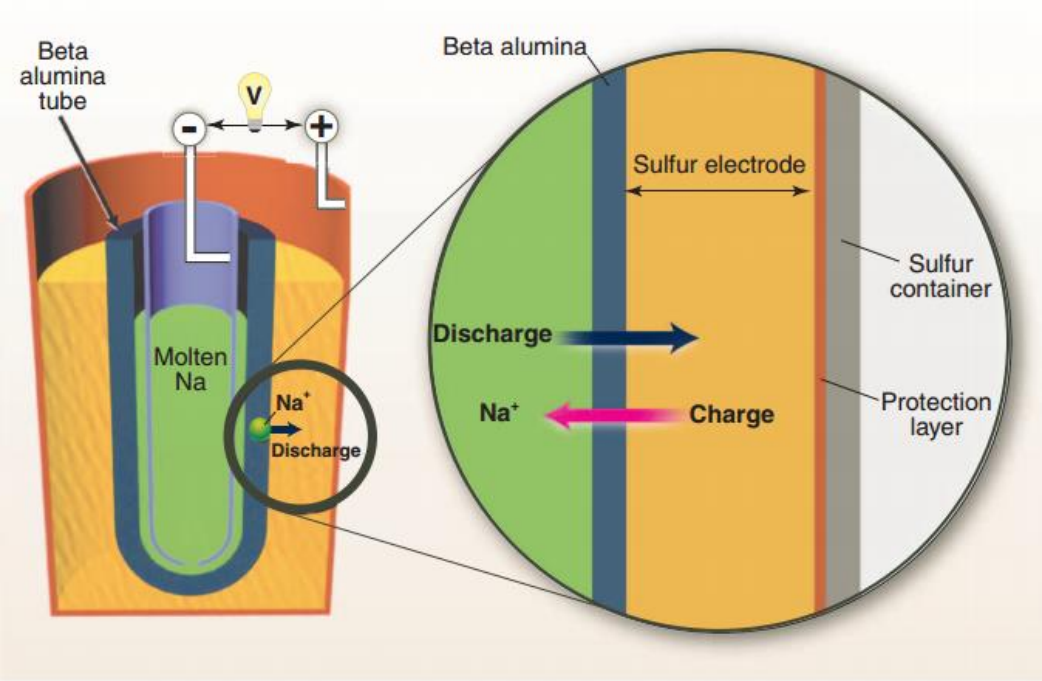

Figure 2. Schematic representation of a high-temperature HT-Na/S battery. Reproduced with permission.[1] Copyright 2011, American Association for the Advancement of Science (AAAS).

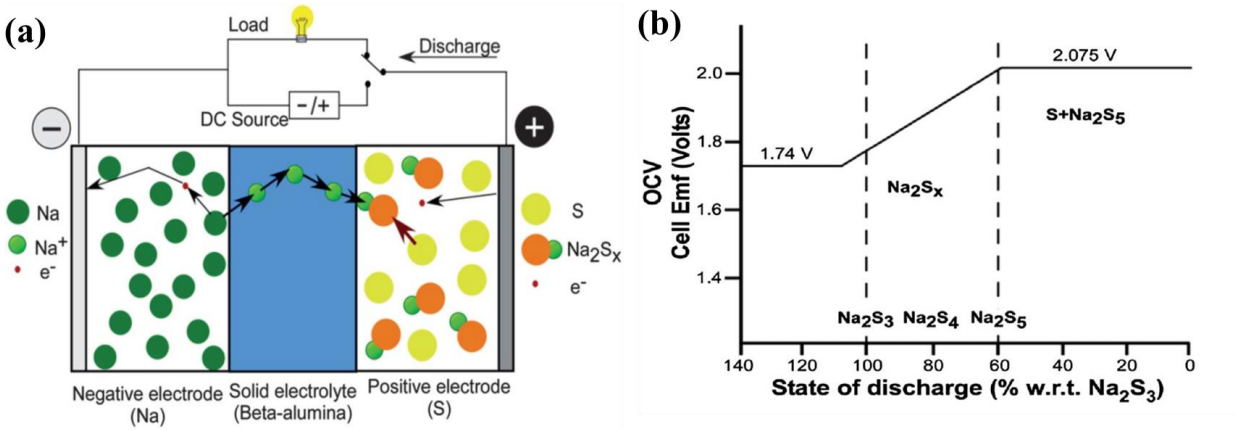

Figure 3. (a) Principle of operation of Na/S cell during the discharge process. (b) Representation of voltage profile of Na/S cell with the various phases present at each stage of discharge. Reproduced with permission.[74] Copyright 2004, Wiley-VCH.

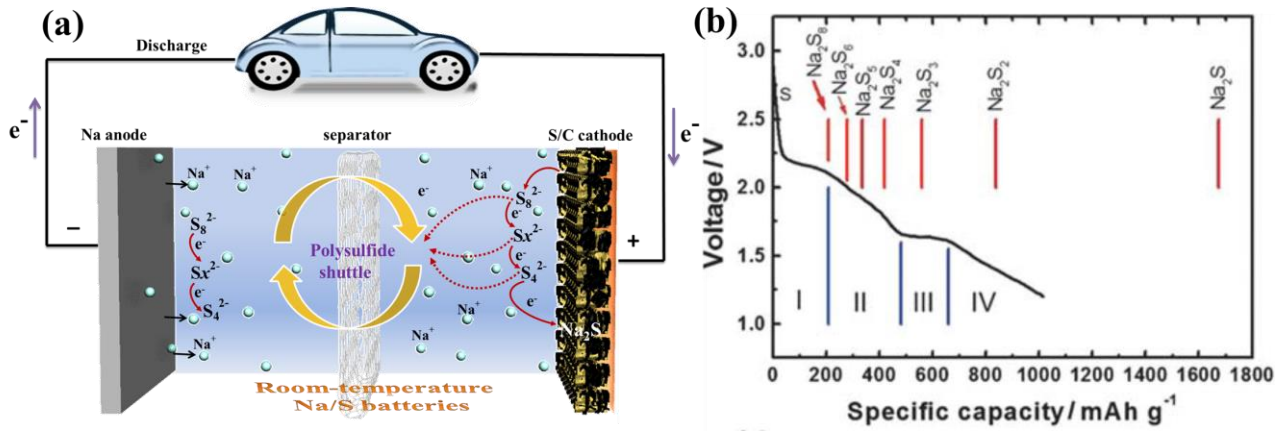

Figure 4. (a) Schematic representation of room-temperature Na/S battery on discharge. (b) Theoretical versus practical discharge capacities of RT-Na/S cells. Reproduced with permission.[78] Copyright 2014, Wiley-VCH.

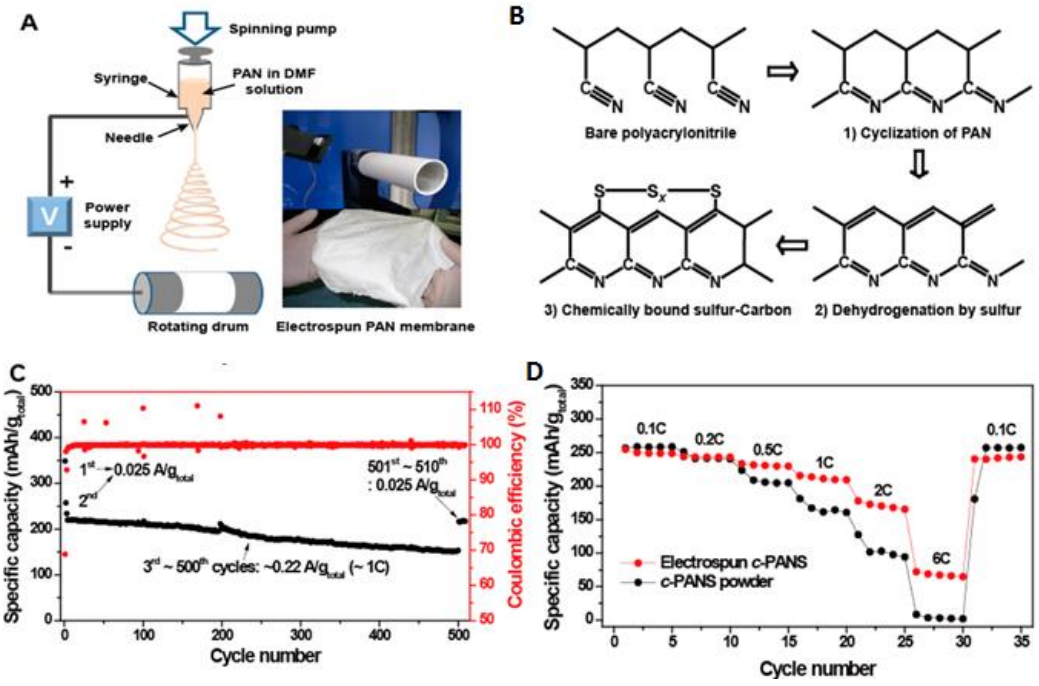

Figure 5. (A) Electrospinning process for the generation of PAN nanofibers. (B) Structural changes during carbonization and sulfurization of c-PANS. (C) Capacity retention and Coulombic efficiency of c-PANS NFs. (D) Rate performances of the electrospun c-PANS NFs and c-PANS powder measured at various C-rates. Reproduced with permission.[58] Copyright 2013, American Chemical Society.

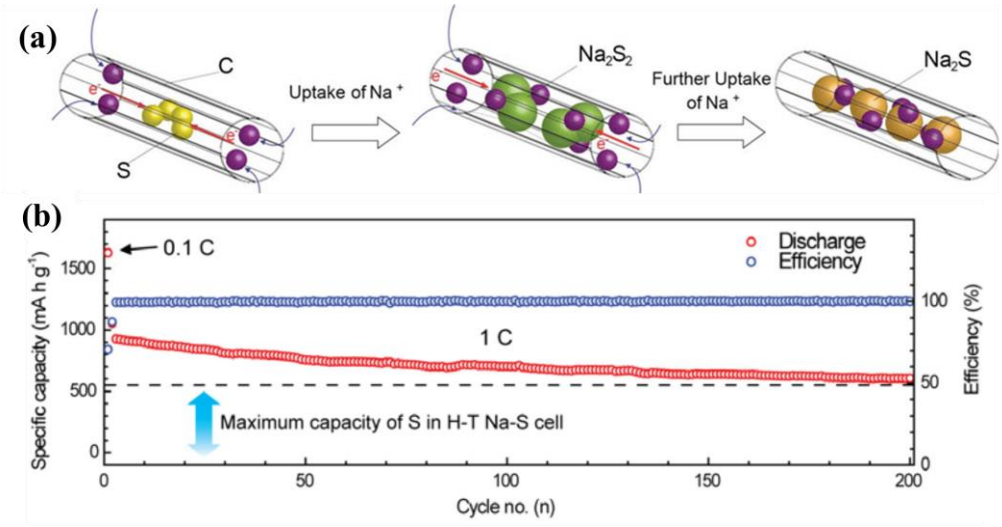

Figure 6. (a) Electrochemical reactions between S and Na^+ during the discharge process. (b) Cycling performance of the S/CNT@MPC cathode at 1 C. Reproduced with permission.[48] Copyright 2014, Wiley-VCH.

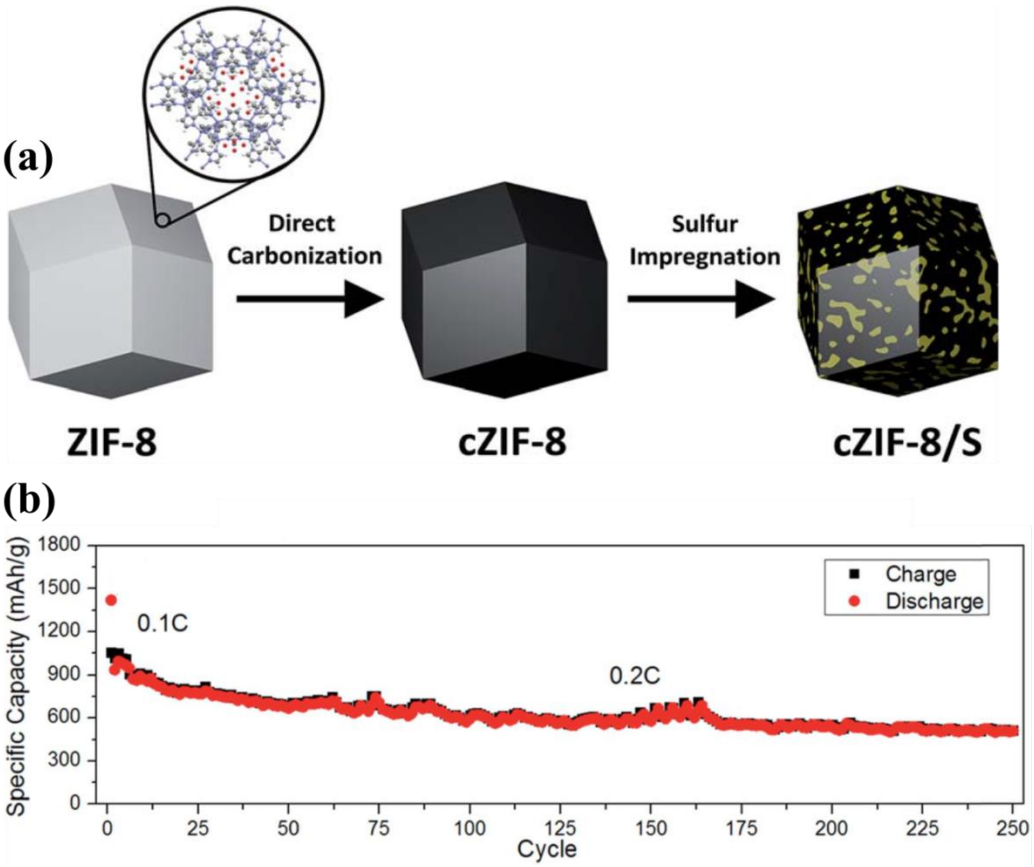

Figure 7. (a) Fabrication procedure for the cZIF-8/S. (b) Long cycle test of Na–S cell at initially 0.1 C for 5 cycles and then 0.2 C up to 250 cycles. The capacity retention after 250 cycles is about 60 %. Reproduced with permission.[86] Copyright 2014, Royal Society of Chemistry.

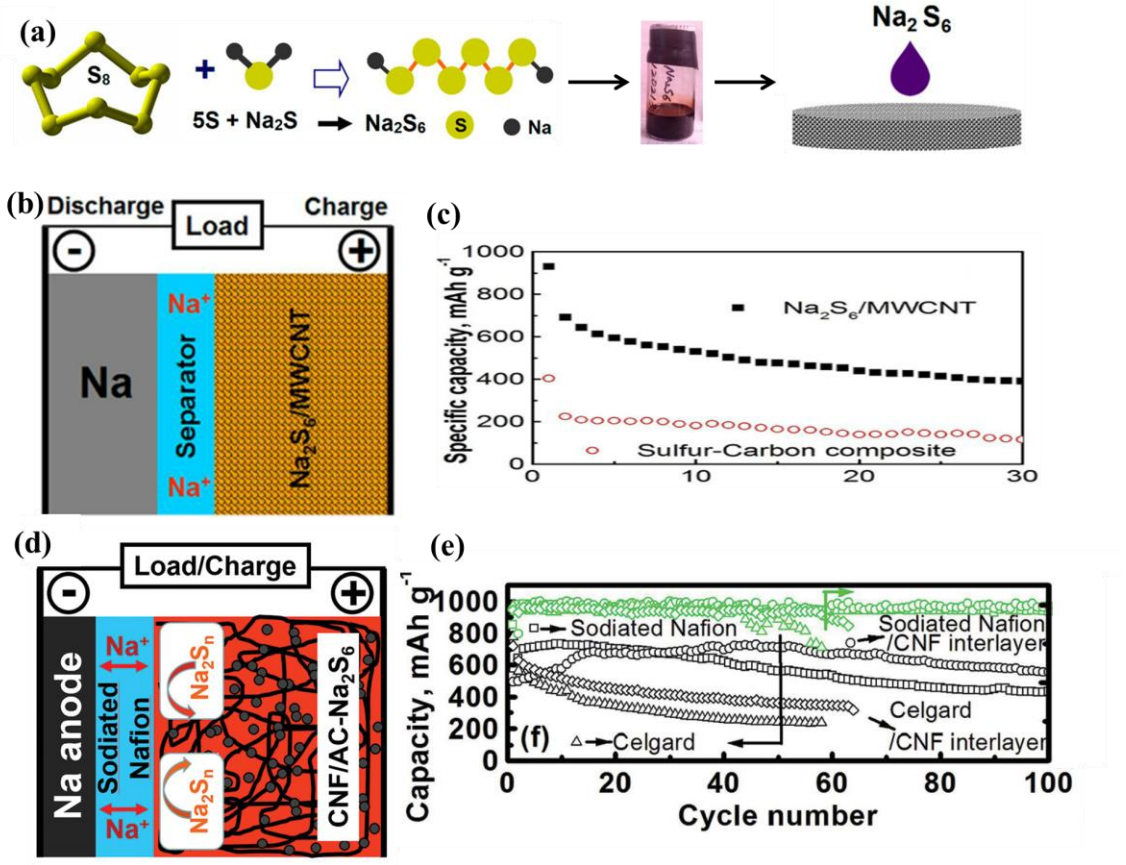

Figure 8. (a) Schematic illustration of the preparation of long-chain Na_2S_6, (b) schematic illustration of a Na/dissolved-polysulfide cell with a MWCNT fabric electrode, (c) cycling performance of the Na/sodium polysulfide cell. Reproduced with permission.[76] Copyright 2014, American Chemical Society. (d) Schematic representation of an RT-Na/S battery with a sodiated Nafion® membrane as a Na-ion selective separator and sodium polysulfide catholyte dispersed into CNF/AC composite as the cathode. (e) Discharge capacities and Coulombic efficiencies of cells with various interlayers. Reproduced with permission.[87] Copyright 2015, Wiley-VCH.

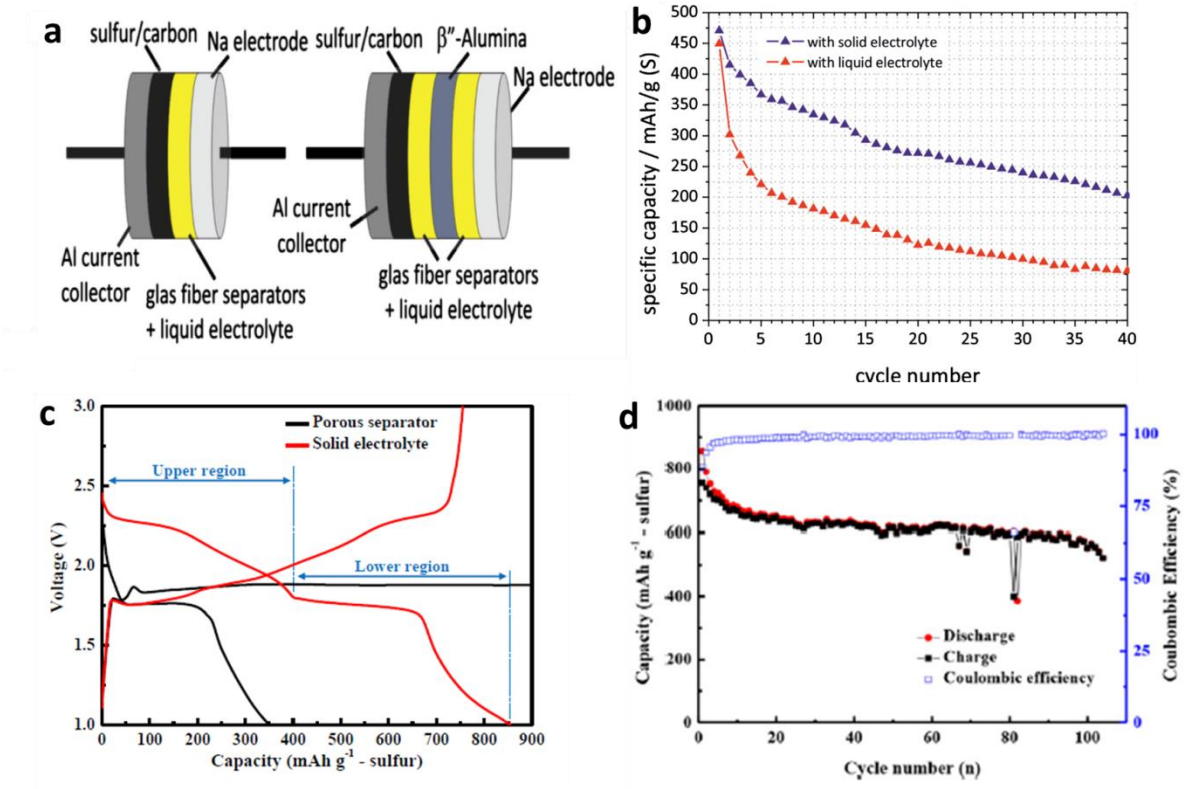

Figure 9. (a) RT-Na/S cells with liquid and solid electrolytes; and (b) discharge capacity as a function of cycle number for the cells with solid and liquid electrolytes, respectively. Reproduced with permission.[47] Copyright 2013, Elsevier. (c) First charge/discharge curves of RT-Na/S batteries with a porous separator and with solid electrolyte; and (d) cycling performance of a Na/S battery with a solid electrolyte over 104 cycles at a current density of 1/64 C (based on sulfur) at room temperature. Reproduced with permission.[94] Copyright 2016, Elsevier.

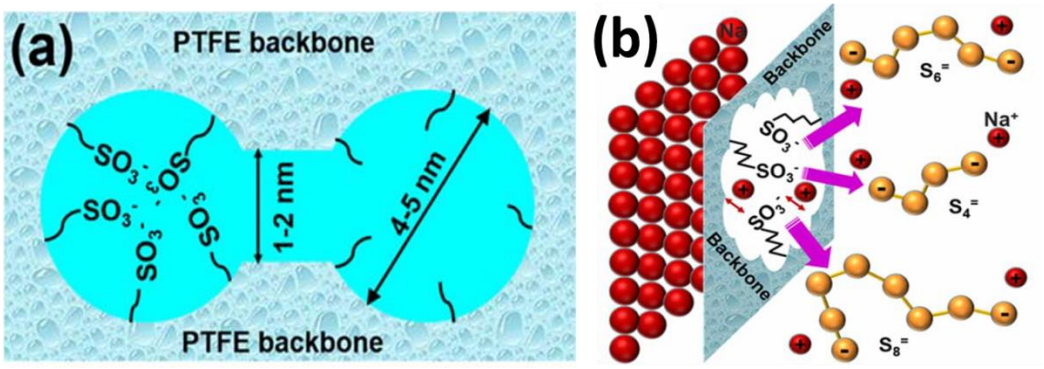

Figure 10. (a) Architecture of Nafion® membrane; and (b) schematic illustration of the ionic selectivity of the Nafion membrane, showing ionic interactions at the hydrophilic pores of the membrane. Reproduced with permission.[89] Copyright 2016, American Chemical Society.

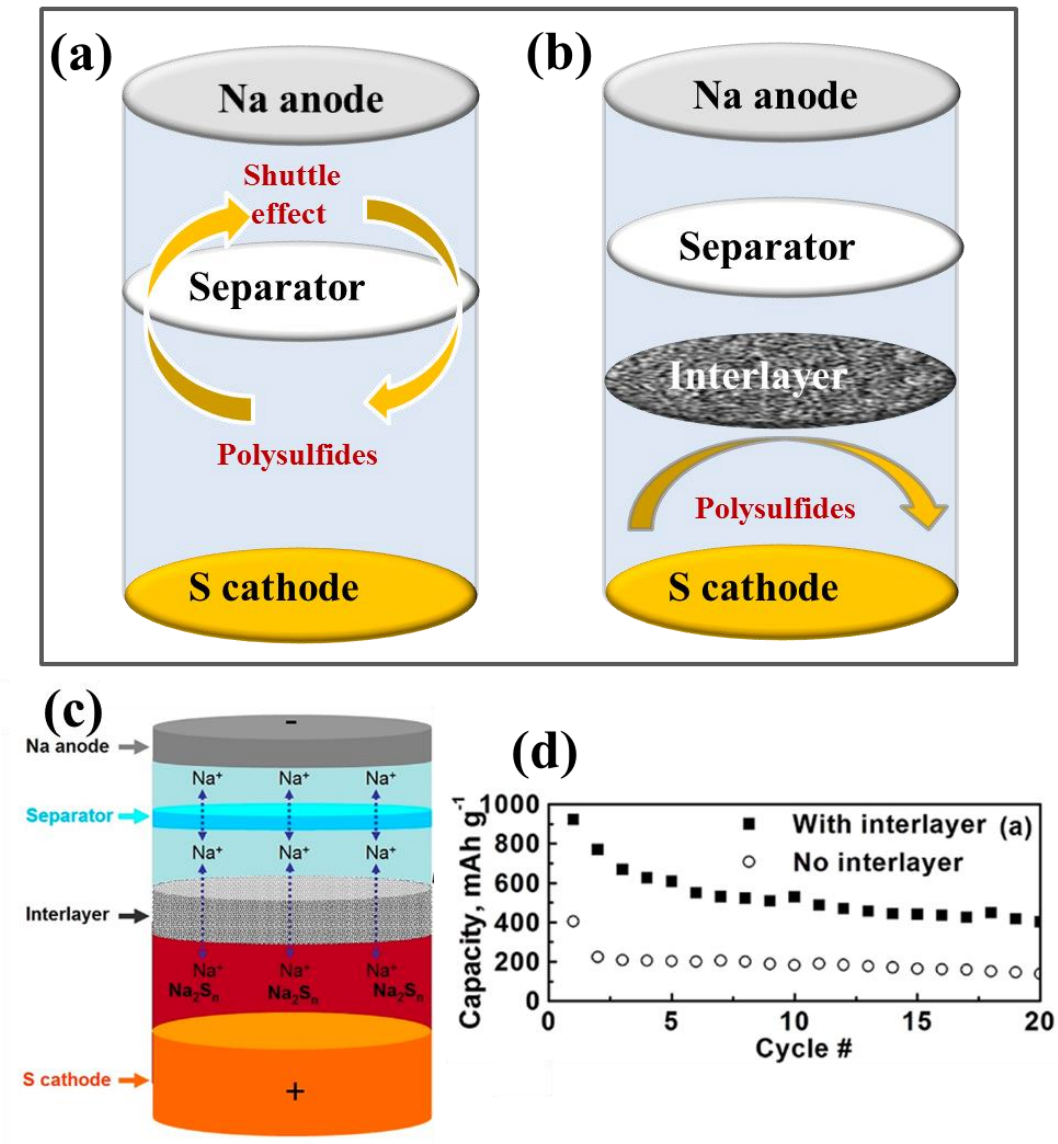

Figure 11. Cell configuration of (a) the traditional cell and (b) a modified cell. (c) Schematic representation of a room-temperature sodium−sulfur battery with an interlayer. The anode, separator, interlayer, and cathode are firmly packed with good mechanical contact, with the spaces between the cell components filled with liquid electrolyte, and the space between the sulfur cathode and the interlayer also filled with polysulfides; and (d) electrochemical characteristics of room-temperature Na/S batteries with and without an interlayer. Reproduced with permission.[77] Copyright 2014, American Chemical Society.

Yun-Xiao Wang is an Associate Research Fellow at the Institute for Superconducting and Electronic Materials (ISEM), University of Wollongong (UOW). She received her Bachelor's degree (2008) from Hebei Normal University and her Master's degree (2011) from Xiamen University. She obtained her PhD degree from the University of Wollongong in 2015. She was awarded a 2017 Discovery Early Career Researcher Award (DECRA) from the Australian Research Council. Her current research interest is renewable energy storage and conversion, including electrocatalysis, lithium/sodium-ion batteries, and lithium/sodium sulfur batteries.

Hua-Kun Liu is a distinguished Professor at the Institute for Superconducting and Electronic Materials, University of Wollongong, Australia, and a Fellow of Australian Academy of Technological Science and Engineering. She received the UOW Vice-Chancellor's Award for Research Excellence as a Senior Researcher in 2013, and won the most competitive ARC Australian Professorial Fellowships in 1994-1998, 1999-2003, 2003-2005, and 2006-2010. She has supervised 62 PhD students to completion and 40 postdoctoral and visiting fellows. Her publications have attracted 25000 citations, H-index: 80. She was selected as highly cited researcher in 2016 (published by Thompson Reuters on 08/09/2016).

Shi-Xue Dou is Distinguished Professor at University of Wollongong. He received his PhD in chemistry in 1984 at Dalhousie University, Canada and his DSc at the University of New South Wales in 1998. He was elected as a Fellow of the Australian Academy of Technological Science and Engineering in 1994. He was awarded the Australian

Government's Centenary Medal in 2003 and multiple Australian Professorial Fellowships. He is a program leader for the Automotive Corporative Research Center-2020. His publications have attracted 21,600+ citations with h-index of 65. He has supervised 80 PhD students, and more than 50 postdoctoral and visiting fellows.